Buller, Casey W., The role of LLT1 (CLEC2D, OCIL) in Ewing sarcoma. Master of Science (Biomedical Sciences), July 2021, 87 pp., 11 illustrations, bibliography, 133 titles

Abstract:

Ewing Sarcoma (EWS) is a pediatric bone cancer that is characterized by a chromosomal translocation giving rise to a neomorphic gene fusion. Although treatment of EWS has a 5-year incident free survival rate of 66%, treatment has plateaued since the 1980's. Natural killer (NK) cells are an important innate immune cell due to their ability to recognize and lyse virally infected and cancerous cells. Unfortunately, cancerous cells often employ strategies such as the downregulation of major histocompatibility complex (MHC) I, or upregulation of inhibitory ligands enabling the escape of T-cells and NK cell mediated killing. LLT1 is an inhibitory ligand our lab had previously shown that it is expressed on TNBC and prostate cancer cell lines. The expression of LLT1 and its function in Ewing Sarcoma (EWS) cell lines has yet to be performed. Our hypothesis is that LLT1 is increased in EWS cell lines TC-32 and CHLA-258 when treated with chemotherapeutic drugs vincristine and etoposide. Our results show that LLT1 is expressed on EWS cell lines and inhibition of LLT1 increases NK cell cytotoxicity. These results indicate that LLT1 is a potential immunotherapy target that needs to be further evaluated in an *in vivo* model.

The Role of LLT1 (CLEC2D, OCIL) in Ewing Sarcoma

Casey Buller, B.S.

Approved:

Major Professor:

Committee Member:

Committee Member:

Committee Member:

University Member:

Chair, Department of Microbiology, Immunology, and Genetics:

Dean, Graduate School Biomedical Sciences:

The Role of LLT1 (CLEC2D, OCIL) in Ewing Sarcoma

Masters Thesis

Presented to the Graduate Council of the
Graduate School of Biomedical Sciences
University of North
Texas Health Science Center
In Partial Fulfillment of the Requirements

For the Degree of

Master of Science

By

Casey Buller, B.S.
Fort Worth, Texas
December 2021

ACKNOWLEDGEMENTS

I would like to thank first and foremost Dr. Stephen Mathew for his mentorship, being patient with me, and giving me guidance when I needed it most. He has been a wonderful mentor and friend; I would not be where I am today without him. I would like to thank my committee Dr. Porunelloor Mathew, Dr. Harlan Jones, Dr. Riyaz Basha, and Dr. Tara Tovar-Vidales for their feedback and support as I took on my project. I would like to thank Dr. Kathleen Borgmann for being my student advisor and always checking up on me and the other CBIM students. Many thanks to Dr. Joseph Malaer for teaching me the basic lab techniques I needed to succeed. I would like to thank my current lab members Michaela Allison, and Luke Cooksey for their friendship and support. I would like to thank the many friends I have made during this time, but I thank Briggs Lambring, Michael Donkor, and Charles Amankwa for being there for me and the many fun conversations we've had. I would like to thank Dr. Rafal Fudala for his technical assistance and use of lab equipment in establishing our cytotoxicity assay. Many thanks go to Dr. Pankaj Chaudhary for his assistance with developing my western blots. A special thanks goes to Dr. Rance Berg, without his teaching and mentorship I would not have thought to join the CBIM program. He has been a wonderful mentor and friend through this program. Lastly, I would like to thank my wife Carley Buller for her constant love and support. She had the courage and trust to follow me to Fort Worth to complete this program and has been my support through it all. She believed in me whenever I did not believe in myself and has gotten me through more than she could imagine. For that, I am ever grateful for you and your love. I would be remiss if I did not thank my dog Estes for staying up with me on late nights and always reminding me to keep a playful spirit even on the bad days. This program has taught me so much about myself and it has been a joy to be a part of the GSBS system.

TABLE OF CONTENTS

LIST OF ILLUSTRATIONS

CHAPTER I

CHAPTER II

CHAPTER III

CHAPTER I

EWING SARCOMA

1.1 Introduction

Cancer is something that continues to plague the lives of many individuals today. Great advances have been made with current standard methods of care (i.e. chemotherapy and radiation therapy), but immunotherapy-based cancer therapies continue to be at the forefront of exciting new research. Ewing's Sarcoma (EWS) is a malignant bone tumor or soft tissue tumor primarily affecting younger individuals twenty years and younger[1]. EWS was first described by Dr. James Ewing in 1921. The disease was described as a "round cell sarcoma" with the presentation of osteomyelitis – a term for inflammation of the bone – but responded well to radium. This was uncharacteristic due to the typical diagnosis of osteogenic sarcoma which did not respond well to radium. Dr. James Ewing noticed this illness followed a pattern in adolescent children – another difference from osteogenic sarcoma. Given X-ray, other histological data, and various case reports, Dr. James Ewing suggested that this disease was separate from osteogenic sarcoma[2]. Later, it would be classified as Ewing Sarcoma – the name being symbolic for Dr. James Ewing who is given credit as the discoverer of the disease. In 2020, an estimated total of 3600 new cases will be diagnosed in the US[3]. Although the five-year survival rate has remained consistent at around 66%, the death rate has remained constant, or plateaued suggesting that new, novel therapies need to be developed[4]. Conventional treatments include surgical resection of the tumor, radiation therapy, and chemotherapy. Current chemotherapy regiments follow the VDC/IE protocol.[5, 6] This protocol alternates between two combinations of the drugs given every two to

three week[6]. The VDC/IE protocol is composed of vincristine, doxorubicin (Adriamycin), cyclophosphamide, ifosfamide, and etoposide[6]. Treatment can be variable in length, but typically ranges from six months to a year. Interestingly, demographic data has been compiled by the US Surveillance Epidemiology and End Results (SEER) registry and upon analysis has found distinct differences between sex and racial disparities[7, 8]. Men accounted for ~60% whereas women accounted for ~40% of all cases[7]. On a global scale, males still show a higher incident rate than women in 10-19 year old children[9]. Broken down between race, ~92% were white, ~2% were black, and ~6% were "other"[7]. The exact cause in sex differences observed remain unclear, but Jawad *et al.* suggest that environmental factors, exposures to specific mutagens, and underlying genetic propensities could contribute to this discrepancy[7]. Birth weight and skeletal growth during puberty have also been proposed, but the evidence supporting these hypotheses provide mixed to little support[10, 11]. Additionally, access to quality healthcare and insurance could be two contributing factors to the lack of reporting in black communities.[12, 13]

On a molecular level, EWS is characterized by a gene fusion occurring between *FET-ETS* regions[1]. The *FET* family of proteins consist of *FUS, EWSR1*, and *TAF15* that are involved in binding to RNA and contribute to the control of transcription, and RNA processing[14]. The *ETS* family of proteins consist of transcription factors that play distinct roles in cellular proliferation, apoptosis, differentiation, lymphoid cell development, angiogenesis, and invasiveness[15, 16]. The most common *FET-ETS* gene fusion is between *EWSR1* (the *FET* portion) and *FLI1* (the *ETS* portion) resulting in a chromosomal translocation t(11;22)(q24;q12)[17]. The *EWSR1-FLI1* fusion accounts for ~85% of EWS cases and result in neomorphic functions by deregulating numerous genes[1, 17]. Although the *EWSR1-FLI1* gene fusion is the most dominant, there are other gene fusion subtypes within the *EWSR1-FLI1* gene fusion. This is dependent on the breakpoint of the

gene fragment either in the intron or exon causing variability between the *EWSR1-FLI1* gene fusion[18]. Additionally, other gene fusions can occur within the *FET-ETS* families of protein. *EWSR1* can fuse to *ERG*, *ETV1*, and *ETV4* among others[1, 19, 20]. These gene fusions are not as common, but the *EWR1-ERG* in ~10% of cases while the others occur in less than 1% of cases[1].

The *EWSR1-FLI1* gene fusion gives rise to a neomorphic protein acts as a transcription factor and oncogene[21]. The neomorphic gene fusion causes upregulation and downregulation of genes such as *DAX-1*, *GLI1*, *FOXO1*, *CCK*, *LOX*, among many others leading to the increased survival of EWS cells[22]. The breadth of dysregulation that *EWSR1-FLI1* causes is due to its ability to retain certain characteristics of its native protein function. The N terminus of the protein is occupied by the *EWSR1* portion which retains its ability to interact with RNA polymerase II and recruit the BAF complex leading to a change from heterochromatin to euchromatin[23, 24]. The C terminus of the protein occupied by *FLI1* retains its DNA binding abilities. In fact, *EWSR1-FLI1* is shown to preferentially bind GGAA-repetitive regions to dysregulate gene expression[25]. Another target of *EWSR1-FLI1* is six transmembrane epithelial antigen of the prostate 1 (STEAP1). Recently, Markey *et al.* showed that NK2 homeobox 2 (NKX2.2) is an important transcriptional co-regulator acting in tandem with *EWSR1-FI1* indicating that *EWSR1-FLI1* cooperates with other transcription factors to dysregulate genes[26]. Although *ESWR1-FLI1* is a neomorphic protein, attempts to target the protein directly have failed due to the inherent instability, lack of enzymatic ability, and lack of a small pocket for a small molecule inhibitor to bind[27]. Instead, targeting transcription factors that interact with *EWSR1-FLI1*, or downstream proteins that are involved with cell signaling that is dysregulated in EWS is an attractive option. Su *et al.* showed that targeting the deubiquitinase OTU domain-containing protein 7A (*OTUD7A*) with a small molecule inhibitor termed 7Ai inhibited EWS

colony formations *in vitro* and *in vivo* providing support for targeting systems that interact with the *EWSR1-FLI1* protein[28]. This indicates the *EWSR1-FLI1* can be targeted indirectly. Additionally, Wang *et al.* showed that pharmacologic inhibition of *EYA3* via Benzarone treatment retards tumor growth and angiogenesis[29]. Briefly put, *EWSR1-FLI1* suppresses miR-708 – which negatively regulates *EYA3* expression[30]. Since the brake in this regulatory network is let off, *EYA3* can promote angiogenesis in EWS, but through pharmacologic inhibition of *EYA3*, the progression of EWS is halted. This provides further evidence of support that targeting downstream influencers of EWS progression can be targeted to promote better outcomes. Thus far, these types of therapies remain to be seen in the clinic, although their efficacy is being evaluated in clinical phase trials[31].

Debate continues with respect to the cell of origin that EWS cells come from. This is complicated by the novel functions that the *FET-ETS* fusion proteins perform. Also, due to the environment where EWS occurs (i.e. bone and soft tissue) potential candidates include cells from the bone mesenchyme, comprising mesodermal and neural-crest-derived cell types[1]. Lack of a definite cell of origin and various neomorphic gene fusions has also led to complications in defining what EWS is and is not. Unfortunately, this creates further categorization dilemmas, and over time the EWS classification has expanded to include EWS, Ewing-like tumors, and small cell round tumors[32]. For the purposes of this study, cell lines (i.e. TC-32 and CHLA-258) will follow Kilpatrick *et al.* definition of EWS that follows the EWSR1 and ETS-family gene fusion molecular event. Under this definition, this includes *EWSR1-FLI1* and *EWSR1-ERG* gene fusion.

Standard treatment options of EWS include chemotherapy, radiation, and surgical intervention. Current research is focused on augmenting treatment options by combining them with targeted immunotherapy, or small molecule inhibitors. Experimental models are not limited

to these constraints, and additional – peculiar – methods do exist. Rademacher *et al.* utilized the power of lentiviral transduction and interleukin-12 (IL-12) to activate the immune – notably NK cells – system to fight EWS[33]. By doing a lentiviral transduction, Rademacher *et al.* induced IL-12 expression anchored to the plasma membrane of A673 EWS cell line and then injected the cells into an NSG and NSG.Tg(Hu-IL-15) mouse. They showed that in both conditions, tumor volume decreased and survival percentage increased in mice injected with A673-LV/hu-IL12 cells[33]. Similarly, they showed that in their NSG.Tg(Hu-IL-15) model produced prolific amounts of IFN-γ, but their NSG mouse model showed minimal production. Conceptually, this delivery system is intriguing since it negates the need to inject IL-12, or other inflammatory cytokines, that may cause an exacerbated response of the immune system. Instead, IL-12 expression is relegated just to the cancerous cells. Intriguing as it is, increased efficacy and safety data needs to be obtained and additional studies need to be performed to determine complete immune activation that occurs since these cells can travel systemically. This study does highlight unordinary measures that are being taken to combat cancers such as EWS. But a multimodal method of attack needs to be employed using standard treatment options, immunotherapy, and other experimental treatments to truly overcome EWS.

Concerning its involvement with the immune system, the EWS tumor mass has a decreased expression of major histocompatibility complex (MHC) I indicating that EWS tumors utilize this to escape immunosurveillance[34]. This is particularly true when metastasis has occurred with a further decrease in MHC I expression[34, 35]. Interestingly, EWS cells lack immune checkpoint molecules like programmed cell death protein 1 (PD1) and programmed cell death 1 ligand 1 (PDL1) indicating that there is a lack of tumor infiltrating lymphocytes (TIL) or that other immunosuppressive mechanisms are employed[36, 37]. Lack of MHC I expression further

indicates that Natural Killer (NK) cells will be an important immunotherapy option based on their innate ability to recognize virally infected or cancerous cells which will be discussed later.

Vincristine belongs to the vinca alkaloids drug group and is derived from the periwinkle plant (*Catharanthus rosea*). Vincristine acts to inhibit the microtubules to further inhibit cellular proliferation during mitosis. It is used to treat multiple cancer types that include leukemia, acute myeloid leukemia (AML), small cell lung cancer, among others. Common side-effects include change in sensation, hair loss, constipation, difficulty walking, and headaches with the potential to cause neuropathic pain, lung damage, and low white blood cell (WBC) counts[38].

Etoposide is a semisynthetic compound that is a derivative of podophyllotoxin. It is extracted from the mandrake root Podophyllum peltatum. Etoposide has potent antineoplastic abilities. Its mechanism of action functions by binding and inhibiting topoisomerase II resulting in the accumulation of DNA breaks. The accumulation of these DNA breaks causes apoptotic death. It is used to treat several types of cancer including testicular, lung, lymphoma, leukemia, neuroblastoma, ovarian cancer, and Ewing sarcoma. Additionally, etoposide is used to treat hemophagocytic lymphohistiocytosis[39]. Although there are multiple drugs used in the treatment of EWS, the aim of this study will be looking specifically at vincristine and etoposide to mimic chemoresistance that occurs during treatment.

Commented [MS1]: ???

The study of EWS *in vivo* remains elusive for a true orthotropic model. Instead, *in vivo* models mainly consist of patient derived cell lines that can be injected into immunocompromised mice to study pulmonary uptake – one prominent metastasis site – but lacks osseous tissue uptake[40]. Although this model can discern some hypotheses, concerns for genetic drift occur for cell lines that are grown in culture among others[41]. 3D scaffolding organoid models can be used, but this still lacks a true *in vivo* system analysis[42, 43]. Patient derived xenograft (PDX) models are

lacking for the study of EWS, but has been suggested as a potential orthotropic model in EWS to study true local and metastasis potential[44]. The quest for a genetic animal EWS model has long been sought after. To date, no such model exists. Although complicated, it is likely due to the role that the *EWSR1-FLI1* gene fusion and the toxicity it elicits during the early stages of mouse development[45]. Theoretically, it would be ideal if the chromosome translocation forming the *EWSR1-FLI1* could be directed, or 'turned-on' at a specific time causing EWS to be inducible. Therefore, it could be a highly controlled model leading to systemic and reproducible models. Unfortunately, this has yet to exist in practice[31, 45].

1.2 Chemoresistance in Ewing Sarcoma

The effects of chemoresistance have been studied throughout various cancer types. In EWS, chemoresistance is the main cause of treatment failure which contributes to why the death rate has plateaued since the 1980's[3]. In general, tumor heterogeneity contributes to chemoresistance through the selection of cancerous cells that are fit to survive in a stress-induced environment. The various intrinsic and extrinsic factors (i.e. epigenetic, transcriptomic, proteomic changes, pH, and hypoxic environment) play a role in picking cancerous cells that are fit to survive these conditions[46]. Chemoresistance can also occur through drug inactivation. A major target for many cancers – including EWS – is the upregulation of glutathione S-transferase family of enzymes. Indeed, high expression of glutathione S-transferase M4 (GSTM4) has been reported in EWS and is correlated with poor patient outcomes[47]. Multiple drug resistance can occur through the difference in gene expression that occurs through induced stress of the cancerous cells. These changes can contribute to the increased release of drugs outside the cell or reduced absorption of the drug[46]. Interestingly, administration of vincristine to SK-ES-1 EWS

cells induced resistance through decreased expression of TUBA1A which is involved in microtubule function[48]. TUBA1A encodes α-tubulin protein which is essential for organizing microtubules during cellular proliferation[48]. Due to resistance of conventional chemotherapy drugs, combination therapies have been studied to determine their efficacy to overcome chemoresistance. Recently, the use of Clotam (Tolfenamic acid or TA) – a small molecule inhibitor – was used in combination with vincristine. This study showed that it increased the anti-proliferative effects of vincristine in EWS[49]. Similarly, a small molecule inhibitor YK-4-279 was used in combination with vincristine. Zöllner *et al.* showed that this combination worked in synergy by inhibiting EWS-FLI1 function in both EWS cell lines and patient-derived xenograft mouse models through the increase of proapoptotic isoforms MCL1 and BCL2[50]. Overall, chemoresistance remains to be the cause of treatment failure in EWS, but targeted therapies are being developed in combination with conventional chemotherapy to overcome resistance and increase survival rates. Another option is to target the immune cells by use of monoclonal antibody treatments to block immunosuppressive cytokines, or to block inhibitory receptors/ligands so that immune cells can become activated to carry out their effector function. Developing a EWS multimodal treatment will be essential to mitigate chemoresistance and increase the survival rate by conversely decreasing the plateaued death rate among pediatric patients.

1.3 The Tumor Microenvironment of Ewing Sarcoma

The tumor microenvironment (TME) is a complex system that aids tumor cells in the suppression of immune cells and harbors an environment that is conducive to the viability of cancerous cells. The TME provides the foundational support from which cancer can survive,

thrive, and metastasize. In the context of Ewing Sarcoma, the TME is in part composed of tumor cells, osteoclast, osteoblast, and stromal cells. Exact composition of the different immune cells that are present in EWS TME has not been performed. Of the immune cells derived from the common lymphoid progenitor, infiltrating T cells make up a large proportion of the present immune cells[51, 52]. The exact composition of NK cells in the TME is unknown, but their composition in other cancers is diminished in comparison to T cell populations[51, 52]. Among T cells, regulatory T cells (T_{reg}) have an immunosuppressive effect on innate and adaptive immune cells. In EWS, T cells with a T_{reg} phenotype ($CD4^+$ $CD25^{hi}$ $FoxP3^+$) are associated with increased metastatic ability highlighting their importance as an immune cell that is utilized by cancerous cells to escape immunosurveillance[53]. Additionally, infiltrating $CD3^+$ T cells are present intratumorally, but EWS cells show a higher expression of HLA-G leading to inhibition and escape from $CD3^+$ T cells[54]. Overall, cancerous cells can utilize immune cells like T_{reg} cells to help modulate immune interactions, but they can also utilize their direct cell-to-cell interactions to modulate the effector functions of immune cells.

In addition to utilizing distinct immune cells to promote a TME that is conducive to escape of immunosurveillance and promotion of cellular proliferation, EWS cells can also secrete cytokines, and other factors that foster a pro-tumor environment. What has been termed the “vicious cycle” is a theory that can be applied to various cancers. Essentially, the tumor provides factors that activate nearby cells. These cells can directly secrete factors, or they can indirectly help secrete factors which lead to further activation of the tumor cells that aid them in uncontrolled proliferation. In the context of EWS, the cancerous cells can secrete factors such as interleukin-6 (IL-6), tumor necrosis factor-α (TNF-α), or parathyroid hormone related-protein (PTH-rP)[55, 56]. These factors activate osteoclast and further drive their differentiation[57-59].

Osteoclast play an important role in the bone environment. They are a bone cell that resorbs, or breaks down, the bone matrix releasing Ca^{2+} among other factors[60, 61]. In the context of EWS, demineralization of the bone matrix leads to secretion of transforming growth factor-beta, (TGF-β), insulin growth factor-1 (IGF-1), and platelet derived growth factor (PDGF) among others[55, 62]. These cytokines and factors can further activate tumoral cells that leads to further proliferation. This process further exacerbates cellular proliferation and osteolysis, hence the name "vicious cycle."

The receptor activator of NF-kappa B ligand (RANKL/RANK) axis cannot be ignored either. Osteoclast activation and differentiation is also mediated by the presence of RANKL when it binds to osteoclast's surface receptor RANK (Figure 1.1)[55, 63]. Osteoprotegerin (OPG) is secreted from osteoblast or osteogenic stromal stem cells that act as a sink for RANKL leading to decreased activation of osteoclast[55, 64]. In the context of EWS, osteoblast cells are repressed leading to a TME that promotes osteoclast activation. Even with repressed osteoblast function, RANKL can still be secreted from other bone cells including EWS derived fibroblast and bone stromal cells further activating osteoclast activation[65]. Overall, the "vicious cycle" is exacerbated giving way to a TME that is conducive to the increased cellular proliferation of EWS cells.

Interestingly, osteoblast possess a cell surface ligand called osteoclast inhibitory ligand (OCIL). This ligand is also called lectin-like transcript-1 (LLT1) which will be discussed in the context of Natural Killer cells later. OCIL was first described on murine cells and *in vitro* studies showed that it works independently of RANKL to regulate osteoclastogenesis during the proliferative phase rather than the differentiation phase[66]. This interaction inhibits osteoclast formation leading to decreased levels and activity of osteoclast. hOCIL was later isolated showing similar effects *in vitro* in human cell lines[67]. There have been no studies looking at

hOCIL expression *in vivo* both in homeostatic conditions, and EWS conditions. In a rat animal model Zheng *et al.*, showed that administration of PTH-rP (1-34) increased rOCIL expression[68]. Indeed, if a similar effect occurs in humans, this is difficult to decipher. PTH-rP is related to increased osteoclast activity, and is secreted from the EWS cells[55, 59]. Yet, PTH-rP also increases rOCIL expression. There are numerous explanations for this, but it ultimately comes down to the lack of studies highlighting the complexities of cellular processes and interactions between multiple cell types.

1.4 The Role of the Immune System in Ewing Sarcoma

Surprisingly, there is little information on the immune cell composition in EWS patients. D'Angelo *et al.*, performed a histological analysis, which showed a minimal amount of tumor infiltrating lymphocytes (TIL) compared to the total amount of cells present, but this represents a single sample[69]. As stated previously, PD-1 and PD-L1 expression is lacking in EWS cells , but in this report, they show that PD-L1 expression is present on macrophages indicating that the TIL's that are present could be subdued by this population of macrophages[37, 69]. Due to the lack of or minimal presence of TIL – specifically $CD8^+$ T-cells – EWS tumors are considered "cold-tumors[70]." However, there are a plethora of variables that determine the immune cell composition in EWS tumors. In general, greater TIL is associated with improved outcomes of survival in various cancers[71-73] In fact, one case report noted that their patient responded to a salvage chemoimmunotherapy combination of paclitaxel (PTX) and Nivolumab (a PD-1 inhibitor) putting forth anecdotal evidence that combinatorial therapy and targeting the immune system can lead to beneficial outcomes[74]. Recent work from several single-sample gene set enrichment analysis (ssGSEA) associate prognostic outcomes with various immune related genes

in EWS, osteosarcoma, and other sarcomas[75-77]. In part, the lack of immune data – especially that of cancerous growth localized to the bone – is due to the absence of an animal model that sufficiently resembles EWS in humans. Thus far, NSG and Nude mice variants have been used, but typically involve metastasis models that do not include the formation of cancerous cells to the bone. Additionally, these models lack certain immune cell subsets making it difficult to gauge the true effect a particular immune cell subsets in a study have. Until a true orthotropic model or additional analysis of EWS samples from patients is performed, the mystery of the immune systems role in EWS will continue to elude researchers.

Even without a true orthotropic model, immune research continues in EWS. The prominent trend with the field of immunotherapy is the formulation and use of chimeric antigen receptor (CAR) T-cells. CAR-T cells are a potent killer of cancerous cells. Ideally, a cancerous cell expressed an antigen or neoantigen that is restricted to EWS cells. Finding an antigen that is specific to EWS is lacking, but there are several antigens being considered for their therapeutic potential such as Insulin-like growth factor (IGF) receptor, LINGO1, and STEAP-1 – among others[78-80]. Indeed, the therapeutic response to CD19 CAR-T cells in patients with B-cell lymphoma has been impressive, but it has failed to translate efficiently to patients with solid tumors[81]. Huang *et al.,* showed that IGF1R and ROR1 CAR T-cells were highly cytotoxic against EWS cells, but their clinical benefit remains to be seen due to the potential of toxicities[82]. An alternative avenue is the use of CAR-NK cells. Kailayangiri *et al.,* constructed a CAR-NK cell against ganglioside antigen GD2 which showed efficacy in clearing EWS expressing GD2, but did not translate into *in vivo* model efficacy[83]. Post-analysis showed that upregulation of HLA-G played a role in EWS tumoral escape and suggest that a multimodal treatment option will be important to have clinical efficacy in these immunotherapies[83].

Figure 1.1

RANK-RANKL-OPG Signaling Pathway

The balance between osteogenesis and bone resorption is governed by the RANK-RANKL-OPG signaling pathway. In brief, Pre-fusion osteoclast express RANK which are activated by binding RANKL which is secreted from osteoblast and osteocytes. Fine tuning of this system also includes the release of the decoy receptor OPG which can bind secreted RANKL and prevents binding to RANK.

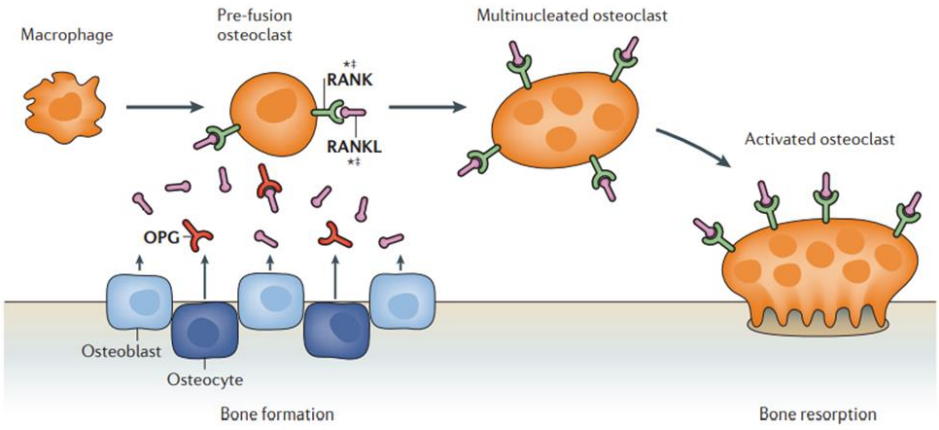

Figure 2 | **Simplified depictions of members of the RANK–RANKL–OPG signalling pathway identified through genome-wide association studies for bone mineral density.** Proteins identified as genome-wide-significant through genome-wide association studies (GWASs) are indicated in bold font and with a bold outline. RANK is encoded by tumour necrosis factor receptor superfamily, member 11a (*TNFRSF11A*), its ligand RANKL is encoded by *TNFSF11*, and the decoy receptor OPG is encoded by *TNFRSF11B*. To generate activated osteoclasts, RANKL is secreted by osteoblasts and osteocytes in bone, and these bind to its natural receptor, RANK, on the surface of pre-fusion osteoclasts. To fine-balance this activation system, osteoblasts and osteocytes also secrete OPG, which is a natural decoy receptor for RANKL and prevents binding of RANKL to RANK. *Indicates the relevance of the gene to human monogenic skeletal disease. ‡Indicates genes with evidence arising from mouse knockouts. The figure is adapted, with permission, from REF. 79 © (2008) Health Plexus Ltd.

Image credit: Richards, J., Zheng, H. & Spector, T. Genetics of osteoporosis from genome-wide association studies: advances and challenges. Nat Rev Genet 13, 576–588 (2012). https://doi.org/10.1038/nrg3228

CHAPTER II

Natural Killer (NK) Cells

2.1 Natural Killer Cells (NK Cells)

Various types of immune cells are involved in the treatment and progression of cancer. One of those cell types that is derived from the common lymphoid progenitor is called the Natural Killer cell (NK cell). NK cells are a fascinating heterogenous group of cells whose function is dictated by the activation and inhibitory signals it receives from the cells that it is interacting which is independent of antigen presentation[84, 85]. It is recognized that NK cell effector functions include their natural cytolytic capacity, antibody dependent cellular cytotoxicity (ADCC), cytokine, and chemokine secretion. Although NK cell receptor expression can be highly variable depending on their maturation state, they are typically divided and described based on their expression of neural cell adhesion molecule (CD56)[86]. As NK cells mature from the hematopoietic stem cells, they gradually lose expression of CD34 (a transmembrane phosphoglycoprotein) and gain expression of CD56[87]. Additionally, acquisition of CD94 commits NK cells to CD56 expression and also acts as an intermediate between $CD56^{bright}$ and $CD56^{dim}$ NK cells[88]. $CD56^{bright}$ and $CD56^{dim}$ NK cells are the two main subpopulations that are focused on when considering NK cell research. $CD56^{bright}$ cells resemble that of T cell lineages that are excellent at secreting cytokines while $CD56^{dim}$ cells resemble the cytotoxic capacity of T cells[89]. Indeed, $CD56^{dim}$ cells are excellent with respect to their cytotoxic capacity in part, due to their expression of CD16 (FcγRIII) that can recognize the fragment crystallization region (Fc) of immunoglobulin G (IgG) family of antibodies[89].

NK cells elicit their cytolytic capacity by the release of perforin, granzymes, and granulysin. Although cellularly complex, the ability to carry out its cytolytic function occurs in

three main processes: (1) target cell recognition, (2) immune synapse formation, (3) and induced death via exocytosis of cytolytic mediators[90]. As suggested in its name, NK cells make great cells for clearing stressed or infected cells. Because NK cells can take in and decipher multiple activating and inhibitory signals it gives them an advantage over T cells in the treatment of cancer. Indeed, T cells are ideal for the direct killing of infected or cancerous cells, but due to lacking specific tumorigenic antigens, NK cells offer a good immunotherapeutic potential. Still, cancerous cells can escape the immunosurveillance of NK cells. This can be achieved by upregulation of inhibitory NK cell receptors, secretion of immunosuppressive factors, and shedding of NK cell receptor ligands[91]. In the case of prostate and TNBC cell lines, there is increased expression of LLT1 – an inhibitory ligand - contributing to decreased clearance of the cancerous cells lines indicating that cancerous cells utilize increased inhibitory NK cell ligands to escape immunosurveillance[92, 93]. Factors such as TGF-β, prostaglandin E_2, indoleamine 2,3-dioxygenase, and adenosine can be secreted from cancerous cells and inhibit NK cell effector functions[94-97]. Shedding of NK cell receptor ligands – such as NKG2DL (MICA, etc.) – leads to decreased expression of NKG2D on NK cells due to over stimulation of the NKG2D receptor[98]. Although cancerous cells have methods to escape NK cell immunosurveillance, great efforts are being made in cancer immunotherapy research to tip the balancing scale from inhibitory to activating signals in NK cells.

Cancer immunotherapy is exciting for two reasons: (1) it utilizes our own immune system to fight off cancerous cells, and (2) the treatment aims to minimize the use of chemotherapy and radiation. Although chemotherapy and radiation have been the standards of care, using such treatments can have unwanted side effects and off target effects. Using NK cells as an immunotherapy platform is interesting because it does not require a specific antigen to target a

cancerous cell and induce its cytolytic effects. Intratumoral NK cell population densities can vary, but increased trafficking to intratumoral sites are correlated with increased survival[99]. This implies that chemokine gradients play a major role in the recruitment of NK cells to the site of the tumor like the CXCR3-CXCR4, CX_3CD1, and CCR3-CCR5 receptor/ligand axis[100]. But higher chemokine serum levels do not necessarily mean that NK cells will effectively be trafficked intratumorally[101]. Several methods to effectively use NK cells as an immunotherapy involved autologous adoptive transfer, CAR-NK therapy, or monoclonal antibodies. Adoptive autologous NK cell transfer means that an individual, or the patient's, own NK cells are isolated from peripheral blood mononuclear cells (PBMC's), expanded *ex vivo*, then transferred back to the patient. This is beneficial since the patient's own blood is being used it does not require the use of immunosuppressive drugs and mitigates the risk of graft-versus-host disease (GvHD). Although beneficial, treatment often fails due to inhibition by self-human leukocyte antigen (HLA) molecules[89]. Chimeric antigen receptor NK cell therapy are similar to CAR-T cell therapy in that the CAR construct consist of an extracellular single-chain fragment variable (scFv) of an antibody directed against a tumor-associated antigen, a hinge region, a transmembrane domain, and an intracellular domain generally composed of the signaling subunits of a costimulatory molecule. Monoclonal antibodies offer a terrific way of targeting specific receptors or their ligands on NK cells or cancerous cells. Because monoclonal antibodies are used, they are specific and will directly target their specified receptor. Additionally, targeting with a monoclonal antibody leads to antibody dependent cell-mediated cytotoxicity (ADCC) by binding to CD16.

Overall, NK cells offer a great platform to be researched as a cancer immunotherapy due to their ability to target cancerous cells based on their expression of inhibitory and activating

receptors. Considerations need to be taken into mind when accounting for how cancerous cells mask themselves from immune cells. Monoclonal antibodies offer novel immunotherapies by their ability to target specific antigens which can lead to direct cytotoxicity or blocking of receptor/ligand binding. Utilizing this can tip the balance back in favor of NK cell cytolytic effector functions leading to increased clearance of cancerous cells. In this study, we will be using an anti-LLT1 antibody to investigate the potential for novel cancer immunotherapy in the treatment of Ewing's Sarcoma.

2.2 Lectin-Like Transcript-1 (LLT1)

Lectin-like Transcript-1 (LLT1, CLEC2D, OCIL) is an NK cell receptor that was first described by Boles *et al.* that is localized on chromosome 12 within the human NK gene complex[102]. Early studies show that the LLT1 receptor is present on NK cells and upon stimulation, increases the IFN-γ secretion from NK cells[103]. Interestingly, this did not affect the cytolytic effect of NK cells to target cell[103]. Additional studies showed that LLT1 is the ligand for NKR-P1A (CD161); a receptor present on NK cells[104, 105]. In the same study, NKR-P1A-LLT1 interaction led to a decrease in cytotoxicity of NK cells to target cells[104, 105]. Elucidation of the crystal structure provides definite evidence for the NKR-P1A-LLT1 interaction with a relatively low binding affinity of *K*d~50μM[106, 107].

LLT1 is present on different immune cells and tissues. Notably, LLT1 is present on circulating B cells and monocytes[108]. To a lesser degree, LLT1 is also present on $CD4^+$ and $CD8^+$ T cells[108]. When immune cells are stimulated, LLT1 expression increases in the $CD4^+$ and $CD8^+$ T cells[108]. LLT1 is also expressed in tissues such as the liver, pancreas, urinary and

digestive tract, and the reproductive system[108]. This suggest that LLT1 plays a role in immune regulation through its interaction with NKR-P1A. LLT1 has been implicated in Rheumatoid Arthritis (RA) due to its expression on macrophages present in the synovial tissue[109]. In the same study, they showed that NKR-P1A expression is increased on T cells and suggested that interaction between the macrophages and T cells will lead to an increase in interferon gamma (IFN-γ)[109]. This suggestion does seem interesting since ligation of NKR-P1A on NK cells leads to a decreased cytolytic effect[104, 105]. Indeed, some studies suggest that NKR-P1A-LLT1 interaction leads to increased IFN-γ secretion in $CD4^+$ $CD161^+$ T cells[110]. Altogether, these studies suggest that the expression of LLT1 can vary depending on if the target cell is in a resting or stimulated state. Additionally, the effect after ligation of LLT1 can be different depending on the cell type furthering implicating LLT1 to have a role in immune regulation.

Interestingly LLT1 expression is also evident in the case of cancer. Our lab has previously shown and characterized the expression of LLT1 on prostate and triple-negative breast cancer (TNBC) cells[92, 93]. In the prostate cancer study, all of the cultured cell lines showed an increased expression of LLT1 (DU145, LNCaP, PC3 and 22Rv1) compared to the non-tumorigenic PWR-1E cell line[93]. Similarly, in the TNBC study, tumorigenic MDA-MB-231 and MDA-MB-436 cell lines showed increased expression of LLT1, while the non-tumorigenic MCF10A did not show increased expression of LLT1[92]. Although blocking of LLT1 via a monoclonal antibody improved NK cell's ability to target and elicit its cytolytic effects, another study suggested that increased LLT1 expression leads to better outcomes in Non-small-cell lung carcinoma (NSCLC)[92, 93, 111]. The study shows that tumor infiltrating lymphocytes (TIL's) were prone to resemble T_h1 cells with respect to their cytokine production such as IFN-γ and tumor necrosis factor alpha (TNF-α)[111]. Overall, these studies further suggest that LLT1 plays a role in

immune regulation with its differential effects on certain immune cell populations. Furthermore, it highlights the significance of LLT1 in cancer. With respect to NK cells, upregulation of LLT1 on cancer cells can be considered an immunotherapy target to tip the balance back to a more activating dominant signal and a subsequent increase in NK cell's cytolytic ability. LLT1's expression, and role in Ewing's Sarcoma has yet to be characterized. Based on preliminary data, LLT1 is expressed in TC-32 and CHLA-258 cells lines with further increased expression of LLT1 when treated with vincristine. Based off previous research done in TNBC and prostate cancer cell lines, it would be interesting to see if blockade of LLT1 reinstates NK cell cytotoxic clearance of EWS cells. Also, in future a xenograft model could validate the *in vitro* findings and provide a rationale for a clinical translational study on a novel LLT1 based immunotherapy.

2.3 NKG2D and DNAM1 in Ewing Sarcoma

NKG2D (CD314) is a cell receptor primarily expressed on cytotoxic immune cells, like NK cells. NKG2D belongs to the NKG2 family of C-type lectin-like receptors and is encoded by the *KLRK1* gene on chromosome 12 in the NK-cell gene complex (NKC)[112]. NKG2D recognize various ligands that include MHC class I polypeptide–related sequence A (MICA), MHC class I polypeptide-related sequence B (MICB), and six members of the UL16 binding protein family (ULBP1, ULBP2, ULBP3, ULBP4, ULBP5, and ULBP6)[113]. Although NKG2D is an activating receptor, stimulation alone of NKG2D is not sufficient to release cytokines, rather NKG2D work in synergy with other activating NK cell receptors to elicit a robust cytolytic response[114].

DNAX accessory molecule 1 (DNAM1, CD226) is a glycoprotein receptor expressed on NK, T cells, and monocytes and is a part of the immunoglobulin superfamily[115]. DNAM1 is an

activating receptor that can bind to poliovirus receptor (PVR, CD155, Necl-5) and Nectin-2 (CD112)[115]. Ligation of DNAM1 causes Fyn-mediated tyrosine phosphorylation and triggering of cytotoxicity in NK cells[116]. Both CD155 and CD112 are upregulated in various cancers indicating that DNAM1 plays an immunoregulatory role[117-119].

Both NKG2D and DNAM1 have been implicated in the context of Ewing Sarcoma as activating receptors that aid in the clearance of cancerous cells[120]. Although chronic engagement of NKG2D soluble ligands (MICA) can decrease the expression of NKG2D on the surface of NK cell, this does not seem to be the case in EWS[98, 121]. In the same study, Berghuis *et al.* showed that expression of NKG2D and DNAM1 receptors were similar regardless of chemotherapy sensitive or resistant cells, but using a histone deacetylase inhibitor and activating NK cells with IL-15 reinstated the cytotoxic effector function[121]. This suggests that inhibitory signaling predominates in NK cell interaction with EWS and that further activation is required to reinstate their cytotoxic function. Additionally, the inhibitory signals that predominate could be due to the increased expression of LLT1 that is present on EWS cells. Combining a multimodal treatment where LLT1 is blocked, and activation of NK cells occurs suggest that there could be increased clearance of EWS cells through NKG2D and DNAM1 dependent mechanisms.

2.4 Hypothesis and Specific Aims

Hypothesis

Chemotherapy drugs enhance LLT1 expression in EWS cells and blocking LLT1-NKRP1A interaction with anti-LLT1 mAb will lead to increased cytotoxicity of EWS cells by NK cells.

Specific Aims

The hypothesis will be tested under the following specific aims.

Specific Aim #1

Determine the expression of LLT1 on EWS cell lines TC-32 and CHLA-258.

Specific Aim #2

Evaluate the cytolytic function of NK cells by blocking LLT1 on EWS cells.

2.5 Significance

Ewing Sarcoma (EWS) primarily effects pediatric patients under the age of 19 years old but is still known to effect adults. EWS is characterized by a chromosomal translocation with the most common translocation occurring between the *EWSR1-FLI1* which causes the dysregulation of multiple genes. Even with conventional therapies such as surgery, chemotherapy, and radiation therapy, the 5-year survival event free incidence has remained steady at 66%. This is highly dependent on whether metastasis has occurred at the time of diagnosis. Metastasis and chemoresistance greatly diminishes the efficacy of treatment with a meager 39% survival rate. Since the 1980's the number of cases has steadily increased while the death rate has plateaued. This highlights the need for new forms of therapy to be developed. Chemoresistance remains a prevailing issue for various cancer types and in EWS it is the main cause of treatment failure. Research into combination therapies to overcome chemoresistance has been done, but their clinical significance remains to be seen, or conducted. Immunotherapies are a promising treatment option due to their ability to target cancerous cells while also promoting an inflammatory response that can counteract the immunosuppressive environment EWS harbors.

Studies have yet to be conducted on the expression and relationship that LLT1 has on EWS cell in relation to NK cells. Current evidence from our lab shows that blocking LLT1 interaction with NKRP1A with a monoclonal antibody tips the balance in favor of increased NK cell cytotoxicity. Therefore, by targeting LLT1 on EWS cells it will tip the balance of activating and inhibitory signals back in favor of activating signals that will allow NK cells to elicit their effector function on EWS. The significance of this study will be to determine the expression of LLT1 on the cell surface of EWS cell lines TC-32 and CHLA-258 and the functional outcome between EWS and NK cells. This will increase our understanding of the role that LLT1 plays in NK cell immunosurveillance and lead to the development of potential target therapies either in combination with current therapies or as a standalone therapy.

Figure 2.1

NK Cell Function

(A) The balance of activating and inhibitory receptors dictates the function effector function of NK cells. Interaction between healthy and NK cells leads to inhibition of the cytotoxic functions of NK cells. (B) The "missing self" is caused by the lack or downregulation of MHC-I complexes leading to an increase in activating signals being received. Lytic granules are directly released to the target cell to lyse it. (C) Stressed or damaged cells can upregulate the cell surface expression of activating ligands. Therefore, whenever a NK cell interacts with the target cell, the increase in activating signals leads to an increase in cytotoxic and lysis of the target cell. (D) Antibody-Dependent Cell-Mediated Cytotoxicity occurs through interaction with the Fc portion of an antibody. The Fc portion binds to the CD16 receptor present on NK cells and leads to direct mediated lysis of the target cell.

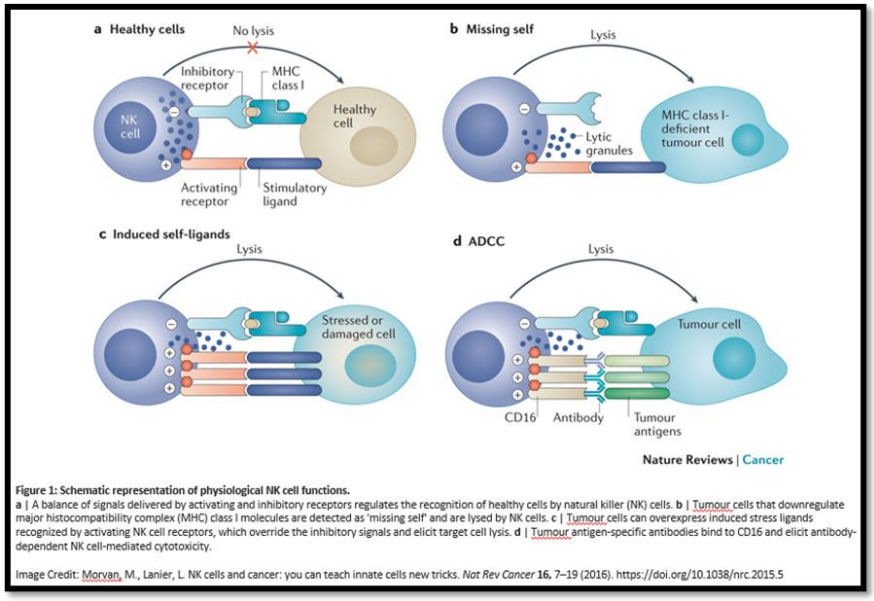

Figure 1: Schematic representation of physiological NK cell functions.
a | A balance of signals delivered by activating and inhibitory receptors regulates the recognition of healthy cells by natural killer (NK) cells. **b** | Tumour cells that downregulate major histocompatibility complex (MHC) class I molecules are detected as 'missing self' and are lysed by NK cells. **c** | Tumour cells can overexpress induced stress ligands recognized by activating NK cell receptors, which override the inhibitory signals and elicit target cell lysis. **d** | Tumour antigen-specific antibodies bind to CD16 and elicit antibody-dependent NK cell-mediated cytotoxicity.

Image Credit: Morvan, M., Lanier, L. NK cells and cancer: you can teach innate cells new tricks. *Nat Rev Cancer* **16,** 7–19 (2016). https://doi.org/10.1038/nrc.2015.5

Figure 2.2

Functional Outcomes of LLT1 Expression

The functional outcome of LLT1 is dependent on which cell it is expressed on. LLT1 is known to interact with NKRP1A (CD161). Previous data from our lab shows that when LLT1 is expressed and upregulated on cancerous cells it leads to decreased cytotoxicity in NK cells which contributes to the escape of cancerous cells from the immune system. LLT1 is also expressed on NK cells and upon stimulation with the L9.7 monoclonal antibody leads to an increase in IFN-γ secretion.

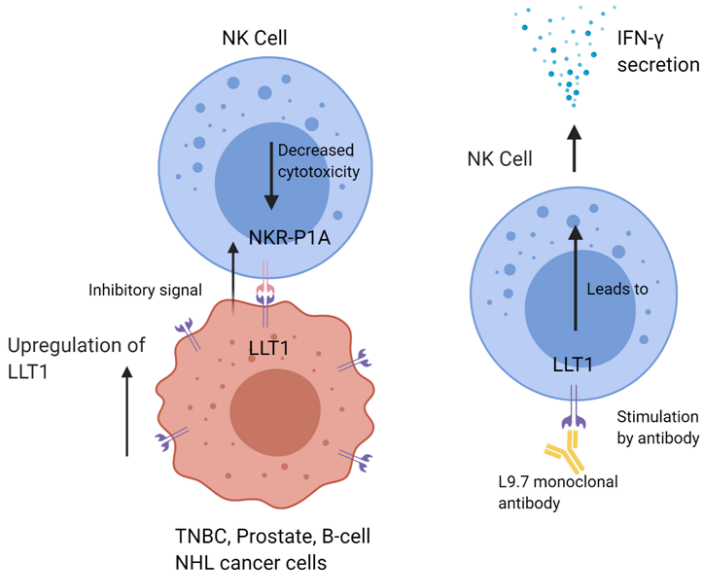

Figure 2: LLT1 is expressed on specific tumor cells such as triple-negative breast cancer (TNBC), prostate cancer, and B-cell non-Hodgkin's lymphoma (NHL) cells. LLT1 on tumor cells interacts with NKR-P1A on NK cells, sending an inhibitory signal to NK cells which decreases cytolytic function. Cancer cells have also been shown to upregulate LLT1 expression to increase the immune dampening effect.

Buller CW, Mathew PA, Mathew SO. Roles of NK Cell Receptors 2B4 (CD244), CS1 (CD319), and LLT1 (CLEC2D) in Cancer. Cancers (Basel). 2020 Jul 1;12(7):1755. doi: 10.3390/cancers12071755. PMID: 32630303; PMCID: PMC7409338.

Figure 2.3

Blocking LLT1-NKRP1A interactions enhances NK cell cytotoxicity

LLT1 interacts with NKRP1A (CD161). Expression of LLT1 on cancer cells inhibits the effector function of NK cells. Blocking LLT1-NKRP1A interactions with a monoclonal antibody leads to lysis by NK cells by blocking inhibitory signals.

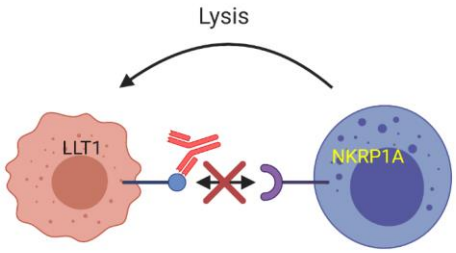

CHAPTER III

MATERIALS AND METHODS

3.1 Cell Lines and Cell Culture

The Jurkat cell line is a non-adherent cell line and was grown in a culture flask containing culture media with Roswell Park Memorial Institute (RPMI) supplemented with 10% Fetal Bovine Serum (FBS), 1 mM sodium pyruvate, 1% amino acids (MEM NEAA), 10 mM HEPES buffer and 100 units/ml penicillin, 100 µg/ml streptomycin, 0.25 µg/ml amphotericin B. TC-32 and CHLA-258 were cultured in Iscove's Modified Dulbecco's Medium (IMDM) supplemented with 10% fetal bovine serum (FBS), 1% Insulin-transferrin-sodium selenite (ITS) media supplement, and 100 units/ml penicillin, 100 µg/ml streptomycin, 0.25 µg/ml amphotericin B. After cells reached confluency of 90-95% they were split and expanded as needed. TC-32 is a EWS cell line (CCR) derived from a 31-month female that had received no prior therapy and possesses the EWSR1-FLI1 translocation. CHLA-258 (CCR) is a EWS cell line derived from a 14-year-old female who had already gone through chemotherapy. The sample came from metastasis to the lung. This cell line also possesses the EWSR1-FLI1 gene fusion. Cell lines were treated with increasing amounts of either vincristine (Sigma Aldrich, cat. # V8879), etoposide (Sigma Aldrich, cat. # 1268808), or a mixture to select for chemoresistant cells. Final concentrations of each drug were determined by performing a viability assay utilizing CellTiter-Glo® Luminescent Cell Viability Assay and plotting of dose response curves to determine the IC50 concentration of each drug. Stock solutions of vincristine and etoposide were

created by dissolving the drug in DMSO and stored in a -200C freezer. Aliquots were thawed and serially diluted to reach desired working concentration of drug in cell culture media.

3.2 Viability Assay

To determine the IC-50 drug concentrations used in this study, a viability assay was conducted using CellTiter-Glo® Luminescent reagent and dose response curves were plotted. In brief, a 96-well plate was used and 100µl of EWS cells (4,000 total cells) were placed in each well. Control wells were established by placing media without cells in appropriate wells. Serial dilutions of VCR and ETO were formulated. VCR concentrations were serially diluted as follows: 2nM, 1nM, 0.5nM, 0.25nM, and 0.125nM. ETO concentrations were serially diluted as follows: 1µg/mL, 0.5µg/mL, 0.25µg/mL, 0.125µg/mL, and 0.0625µg/mL. Drugs were incubated with cells overnight. The following day 100µl of CellTiter-Glo® Luminescent reagent was added and mixed for 2 minutes on a plate shaker. The plate was then incubated at room temperature for 10 minutes. Luminescence was then recorded on a 96-well plate reader. A log-transformed curve was established to determine IC-50 concentration.

3.3 Real Time Quantitative Polymerase Chain Reaction (RT-qPCR)

RNA from treated and non-treated cell line was isolated using TRIzol (Invitrogen cat. # 15596026) reagent, converted into cDNA constructs, then amplified using TaqMan primers to determine C_T values and compare the fold expression increase in treated and non-treated cell lines compared to a control cell line. Briefly put, $5*10^6$ cells were spun down at 250Xg for 5 minutes. TRIzol was added and let sit for 5 minutes. Chloroform was added and shaken

vigorously for a brief period. Samples were incubated at room temperature for a brief time then centrifuged at 12,000Xg for 15 minutes at 4ºC. After this, three distinct layers of separation were visible. The clear (top) layer was pipetted out and placed in a new Eppendorf tube. In the new tube 100% isopropanol was and incubated at room temperature for 10 minutes. Samples were then centrifuged at 12,000Xg for 15 minutes at 4ºC. Supernatant was removed and washed in 75% EtOH then centrifuged at 7500Xg for 5 minutes at 4ºC. Supernatant was decanted off then let dry in a Laminar Flow hood for no longer than 20 minutes. RNA was resuspended in RNase-free water (DEPC-treated water) and vortexed to ensure proper reconstitution. Samples were incubated on a heat block at 55-60ºC for 10-15 minutes. RNA samples were checked for concentration and purity using a NanoDrop (Thermo Scientific, cat. # ND-2000C).

cDNA conversion immediately followed RNA isolation using a High-Capacity cDNA Reverse Transcription Kit with RNase Inhibitor (Applied Biosystems, cat. # 4374966). A maximum amount of 2µg of total RNA was used in a 20µl reaction setup. A reverse transcriptase (RT) master mix (MM) was made per supplier's protocol. 10µl of the MM was mixed with 10µl of RNA sample, mixed by pipetting up and down, then transferred to a new microcentrifuge tube. A programmable thermocycler was used following supplier's protocol. Samples were either immediately used to perform RT-qPCR or stored at -15 to -25ºC.

RT-qPCR was performed using a StepOnePlus Real Time PCR-System (Applied Biosystems, cat. #4376357). Briefly put, 15ng of cDNA was used and mixed with either TaqMan Gene Expression Assay LLT1 or GAPDH primers, RNase-free water, and TaqMan Gene Expression Master Mix to have enough to make quadruplicates. Once ready, 20µl of sample was placed in a 96-well reaction plate, sealed, centrifuged briefly, then placed into the StepOnePluse system and ran. Samples were normalized to the Jurkat cell line.

3.4 Western Blot

Western blot was used to detect protein presence in treated and non-treated samples. Briefly put, cell samples were grown out to 90-100% confluency then washed with 1XPBS+1mM EDTA. Then the cells were treated with RIPA buffer treated with a phosphatase and protease inhibitor and incubated on ice for a short period. The cells were then aspirated with the same RIPA buffer and transferred to a separate tube. Spin down at 16,000Xg for 30 minutes and transfer the supernatant to a separate tube and placed on a heat block at 95^{o}C for 10 minutes then determined the protein concentration using a Thermo Fisher NanoDrop.

Samples were then prepared to load into a premade Bis-Tris gel (Invitrogen cat. # NP0321BOX). The samples were mixed with a non-reducing sample buffer (Thermo Scientific cat. #84788) and autoclaved H_2O. A total of 20µg of protein sample was used and loaded. Presharp Prestain and MagixMark XP Western Protein standard (Invitrogen cat. # LC5602) was prepared and loaded. The gel was placed in a XCell SureLock™ Mini-Cell (Invitrogen cat. #EI0001). A working 1X solution of MOPS running buffer was prepared. The gel was run at 200V for ~60 minutes then placed in an iBlot 2 Transfer Stacks, nitrocellulose membrane (Invitrogen, cat. # IB23001) and transferred using the iBlot 2 Dry Blotting System (Invitrogen, cat. # IB21001). The nitrocellulose membrane was removed and blocked using the StartingBlock™ T20 (TBS) Blocking Buffer (Thermo Scientific, cat. # 37543) for 1 hour. Goat anti-human LLT1 primary antibody (R&D Systems, cat. # AF3480) incubation followed by performing a 1:1000 dilution in StartingBlock™ T20 (TBS) Blocking Buffer (Thermo Scientific, cat. # 37543) overnight at 4^{o}C with constant rocking. The next day the membrane was washed three times with StartingBlock™ T20 (TBS) Blocking Buffer (Thermo Scientific, cat. # 37543).

Donkey anti-Goat IgG HRP conjugated antibody (R&D Systems, cat. # HAF109) and HRP Donkey anti-rabbit IgG antibody (BioLegend, cat. #406401) were diluted at 1:1000 dilution and incubated at room temperature for 1 hour. Membrane was washed three times. Pierce™ ECL Plus Western Blotting Substrate (Thermo Scientific, cat. #32132) at a 1:1 solution then imaged using a chemiluminescence western blot reader. Membranes were re-probed with Direct-Blot™ HRP anti-GAPDH Antibody (BioLegend, cat. # 649204) for 1 hour at room temperature then detected using ECL substrate.

3.5 Flow Cytometry

Cells were harvested, centrifuged at 250Xg for 5 minutes then resuspended in 5mL of 1XPBS+BSA. Cells were counted on the Denovix Cell Drop using Trypan Blue staining to analyze live cells. An adequate number of cells were taken so that sample tubes had $1*10^6$ cells total per tube. The cells were incubated with Fc block (1µL per $1*10^6$ cells) for 5 minutes then divided up into the appropriate sample tube. The primary antibody LLT1-PE (R&D, cat. # FAB3480P) (5µL per $1*10^6$ cells) and anti-mouse IgG1-PE (BioLegend, cat. # 406607) (5µL per $1*10^6$ cells) was added to each of the appropriate tubes. Primary antibody incubation occurred for 30 minutes at 4^oC in the dark. Samples were then washed (250µL) twice at 250Xg and resuspended in 50µL 1XPBS+BSA. Samples were resuspended in 150µLAnnexin-V Binding Buffer then incubated with Annexin-V and 7AAD (5µL per sample, each) per suppliers' recommendation (BioLegend, cat. # 640922) and incubated in dark for 15 minutes. An additional 200µL of Annexin-V Binding Buffer was added to each sample then transferred to flow tubes. Appropriate single stain positive controls and negative controls were prepared. Samples were

placed on ice until ready to run either on BD LSR II or Amnis ImageStream MK II Imaging Flow Cytometer.

3.6 Isolation of Human Peripheral Blood Mononuclear Cells and Primary Natural Killer Cells

Peripheral blood mononuclear cells (PBMCs) were isolated from whole blood obtained from healthy human subjects with informed consent and prior approval by the Institutional Review Board (North Texas Regional IRB # 20-28). Primary natural killer cells were then isolated from PBMCs. Whole blood was collected from healthy volunteers using Acid dextrose vacutainer tubes (BD cat. #364606) and was layered on top of Histopaque-1077 (Sigma Aldrich cat. #10771) density gradient. The Histopaque-1077 density gradient was used to separate whole blood into different layers (serum, PBMCs, platelets, and erythrocytes layers). Samples were centrifuged in a 50mL Leucosep (Greiner Bio-One cat. #89048-932) tube for 20 mins. After centrifugation, the white layer consisting of PBMCs was carefully isolated into new sterile 50 mL conical tubes and processed further according to PBMC purification protocol. Upon isolation of PBMCs, PBMCs were counted using the Denovix Cell Drop to determine total cell count to proceed with the following isolation of NK cells. Primary natural killer cells were isolated from PBMCs by following standard protocol instructions in the Miltenyi Biotec NK cell isolation kit (Miltenyi, cat. #130-092-657). In brief, PBMCs were treated with a prepared buffer consisting of phosphate-buffered saline (PBS at pH 7.2), 0.5% bovine serum albumin (BSA), and 2 mM EDTA. NK cell biotin-antibody cocktail was, then, added to the buffer-treated PBMCs and underwent a 5-minute incubation at 4ºC. After incubation, PBMCs were treated with NK cell microbead cocktail before the subsequent magnetic NK cell separation step. In theory, lymphocytes except NK cells are labeled with the magnetic beads. Once the sample is run

through the column and subjected to a magnetic field, the NK cells can be collected as the flow through while the remaining lymphocytes remain in the column. Primary NK cells were cultured in 4+ RPMI media supplemented with 10% fetal bovine serum in a fresh culture flask.

3.7 DELFIA Cytotoxicity Assay

PBMC's were isolated prior to starting cytotoxicity assay following suppliers' protocol (Miltenyi, cat. #130-092-657). NK cells were placed on ice until EWS cells were prepped. EWS cells were grown out in a culture flask until 90-100% confluent. Cells were harvest and resuspended in 5mL of 1XPBS+BSA, transferred to a 15mL conical tube and counted on a Denovix Cell Counter using the Trypan Blue viability stain. NK cells were incubated with Fc block (1µL per $1*10^6$ cells) then suppliers' protocol was followed to carry out the remainder of the experiment (Perkin Elmer, cat. #AD0116). In brief, after counting the cells the concentration of cells was adjusted to $1*10^6$ cells per mL and a total volume was adjusted to 2-4mL in fresh IMDM media. Each sample tube was incubated with 5µL of the BATDA reagent and incubated in an incubator at 37^0C, and 5% CO_2 for 30 minutes. After the incubation period, the samples were washed twice and spun down at 250Xg for 5 minutes each resuspended in fresh IMDM media. The volume was adjusted to 5000 cells per 100µL in fresh IMDM media. 100µL of solution was pipetted into a V-bottom 96-well plate sufficient to perform triplicates of your samples. Various ratios of E:T were used (i.e., 25:1, 5:1, and 1:1). Effector NK cells were resuspended in 4+RPMI media and serially diluted so that one tube has 125,000, 25,000, and 5000 cells per 100µL. The appropriate number of cells were pipetted out in triplicate and co-incubated with the EWS cells for 2 hours at 37ºC and 5% CO_2. After the 2-hour incubation the 96-well plate was taken and centrifuged at 250Xg for 5 minutes. 20µL of the supernatant was

taken from each well and placed in a new flat bottomed 96-well plate. Then it was mixed with 200µL of Europium solution for 15 minutes with constant agitation on a plate shaker covered. The plate was then read on a BioTek Cytation 3 machine taking readings at excitation wavelength 340nm and emission at 615nm. Control wells included 100% lysis control well which contained EWS sample cells post-BATDA incubation and 10µL of supplier provided lysis buffer. Spontaneous release included EWS cells post-BATDA incubation in media only. Background noise was determined by plate wells that contained a 1:1 mixture of IMDM and RPMI media.

CHAPTER IV

RESULTS

Specific Aim #1: Determine the expression of LLT1 on EWS cell lines TC-32 and CHLA-258.

Rationale

Lectin-Like Transcript-1 (LLT1) is a ligand that is present on NK cells, healthy tissues, and is known to be expressed on different cancer types like triple negative breast cancer (TNBC), prostate cancer, and B-cell non-Hodgkin's lymphoma (NHL). LLT1's natural ligand is NKR-P1A (CD161), which is present on NK cells, among other immune cells. When LLT1 binds to NKR-P1A, an inhibitory response occurs in NK cells, which decreases its cytotoxicity whereby lysis of the target cell does not occur. In the context of cancer, this is bad because it allows cancerous cells to escape NK cell immunosurveillance. Previous research has shown that LLT1 is present on cancerous cell lines including TNBC, prostate, colon, and B cell NHL. So far, there is no published research on the expression of LLT1 on EWS. The objective of this aim is to characterize the expression of LLT1 on EWS, and does treatment of EWS cell lines with vincristine and etoposide increase expression of LLT1. The working hypothesis is that chemotherapy drugs increase expression of LLT1 on EWS cells to prevent activation of NK cells thereby contributing to escape of NK cell immunosurveillance.

4.1 Ewing Sarcoma Cell Lines Express Lectin-Like Transcript 1 (LLT1)

4.1.1 Establishing IC50 concentrations

Several reports indicate that LLT1 is expressed on other cancers[92, 93]. Here we have investigated the expression of LLT1 in EWS cells and how the treatment of chemotherapy drugs vincristine (VCR) and etoposide (ETO) effect the expression of LLT1 in EWS cells. IC-50 concentrations of the drugs were determined by treating the EWS cells with different concentrations of vincristine and etoposide and analyze the cell viability utilizing CellTiter-Glo® Luminescent reagent. A 96 round bottom well plate was used and 100µl of EWS cells (4,000 total cells) were placed in each well. Serial dilutions of each drug was used, and the cells were treated at different concentrations. After the incubation period, the CellTiter-Glo® Luminescent reagent was added and the fluorescence was measured. Data was analyzed to form a log-transformed curve to determine the IC-50 concentration. TC-32 VCR IC-50 concentration was 0.38nM and TC-32 ETO IC-50 concentration was 0.20µg/ml (Figure 4.1). Although TC-32 IC-50 concentration was 0.38nM, the TC-32 cell line was treated at 0.5nM VCR concentration indicating that these are highly chemoresistant cells. CHLA-258 VCR IC-50 concentration was 0.43nM and CHLA-258 ETO IC-50 concentration was 0.14µg/ml (Figure 4.2). CHLA-258 VCR cells were also treated at 0.5nM VCR concentration indicating these are highly chemoresistant cells. Although not tested using the cell viability assay, a combination of VCR and ETO was used to investigate the effect of combinatorial treatment of EWS cell lines has on LLT1 expression. Cell lines were progressively treated to their 0.5nM concentration then 0.5µg/ml of ETO was added. Both the cell lines were treated for 2 weeks before experiments were done to select for true chemoresistant cells.

4.1.2 Increased mRNA expression in non-treated EWS cell lines

RT-qPCR analysis were conducted to determine the mRNA expression of LLT1 in vincristine and etoposide treated cell lines compared to non-treated cells. RNA isolation was performed using the TRIzol reagent with subsequent cDNA conversion. Utilizing TaqMan primers, LLT1 was amplified for a total of 45 cycles. The Jurkat cell line has little to no expression of LLT1 and was used as the control to normalize the data against. Fold expression change in RNA was determined using the ΔΔCt method indicating the increase or decrease in a gene of interest against the control cell line. TC-32, TC-32 VCR, and TC-32 VCR/ETO values were 0.6-, 0.35-, and 0.05-fold expression change, respectively. CHLA-258, CHLA-258 VCR, CHLA-258 ETO, and CHLA-258 VCR/ETO values were 0.78-, 0.45-, 0.21-, and 0.21-fold expression change, respectively (Figure 4.3). A students t-test was used to analyze the results of the data with a significant value set at $p<0.05$ and $p<0.001$. Statistical analysis showed TC-32, TC-32 VCR, and TC-32 VCR/ETO were all significant at $p = 0.038$, 0.039, and 0.018, respectively. CHLA-258 and CHLA-258 VCR were significant at $p = 0.033$ and 0.048, respectively. Both CHLA-258 ETO and CHLA-258VCR/ETO were non-significant, but trending towards significance at $p = 0.053$ and 0.067, respectively. These results indicate that there is mRNA expression of LLT1 in EWS cells, but in both cell lines the total mRNA expression in treated cells is decreased as compared to non-treated cells.

4.1.3 Treated EWS cell lines do not show a change in total LLT1 protein expression.

5 million TC-32 and CHLA-258 cells were harvested and lysed with lysis buffer and the cell lysate was ran on an SDS-PAGE Bis-Tris gel at 200V for 60 minutes then transferred to a nitrocellulose membrane where they were blocked and probed with an anti-LLT1 antibody and then probed with a horse-radish peroxidase (HRP) secondary antibody. The membrane was then exposed to ECL substrate and imaged. After imaging the membrane was stripped and re-probed with an anti-GAPDH-HRP conjugated primary antibody. The membrane was exposed to ECL substrate and imaged. Western blot analysis indicates that treated cell lines do not show a change in total protein concentrations of LLT1 as compared to non-treated cell lines (Figure 4.4). The quantification of band intensity shows that the untreated TC-32 and TC-32 treated with VCR showed almost identical LLT1 expression whereas there was a slight decrease in the LLT1 protein concentration in the cells treated with both VCR and ETO. CHLA-258 showed the highest LLT1 expression. TC-32 ETO, CHLA-258 VCR, CHLA-258 ETO, and CHLA-258 VCR/ETO samples were also ran, but protein expression was not detected.

4.1.4 LLT1 is expressed on the cell surface of TC-32 and CHLA-258 and treatment with vincristine further increases the expression.

Cell samples were harvested and counted with a Trypan Blue viability staining. The appropriate number of cells were taken and incubated with Fc block. Then the samples were incubated with either isotype control or LLT1-PE antibody. Samples were incubated with Annexin-V and 7-AAD next then placed on ice until ready to run flow cytometry. Flow cytometry analysis indicates that LLT1 is expressed on the cell surface of both EWS cell lines as determined by mean fluorescent intensity ratio (MFIR) which is a ratio of the MFI that compares expression of target of interest. Our initial experiments showed that TC-32 and CHLA-258 had

cell surface expression with a MFIR of 1.3 and 1.5, respectively. TC-32 treated with VCR and CHLA-258 treated with VCR showed a MFIR of 2.5, and 1.3, respectively. Flow analysis showed an increased expression of LLT1 in TC-32 treated with VCR ($p= 0.038$) compared to the non-treated TC-32 cell line (Figure 4.5 & 4.6). Treated cell lines TC-32 ETO and TC-32 VCR/ETO had increased expression of LLT1 but decreased expression in comparison to TC-32 VCR. These were single, independent, experiments due to these samples lack of viability. CHLA-258 VCR treated cell line had an increased expression of LLT1 compared to the non-treated cell line but lacked significance ($p= 0.057$). CHLA-258 ETO and CHLA-258 VCR/ETO treated cell lines had decreased cell surface expression of LLT1, but comparable to CHLA-258 LLT1. CHLA-258 ETO and CHLA-258 VCR/ETO were also single, independent, experiments due to lack of cell viability. A One-way ANOVA confirmed differences in the means of MFIRs at $p<0.05$ for all cell lines. Dunnett's multiple comparison post-hoc was used to test for statistical significance of MFIRs compared to the control TC-32 and CHLA-258 non-treated cell lines (* $p<0.05$, ** $p<0.001$).

Figure 4.1

Dose response curves to determine IC-50 concentration of TC-32 EWS cell line

CellTiter-Glo® Luminescent reagent was used to perform a cell viability assay. VCR was diluted at 2nM, 1nM, 0.5nM, 0.25nM, and 0.125nM in IMDM media and incubated with 5000 TC-32 cells per well. ETO was diluted at 1µg/mL, 0.5µg/mL, 0.25µg/mL, 0.125µg/mL, and 0.0625µg/mL.in IMDM media and incubated with 5000 TC-32 cells per well. The 96 round bottom plate was analyzed using a plate reader. Data was log-transformed to standard curve to determine the IC-50 concentration of VCR and ETO.

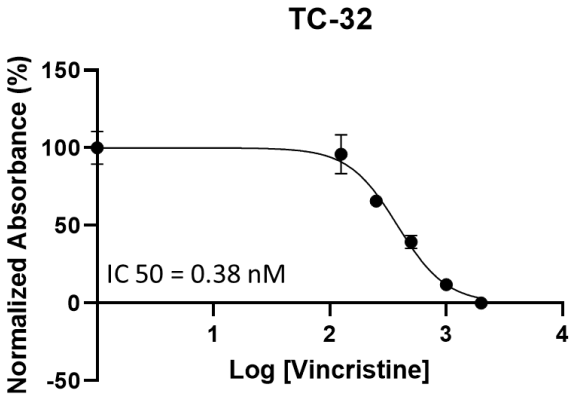

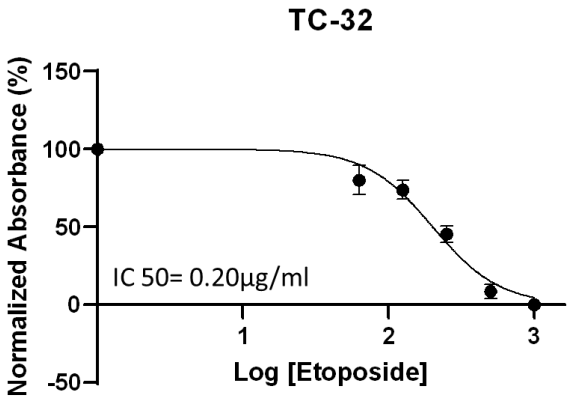

Figure 4.2

Dose response curves to determine IC-50 concentration of CHLA-258 EWS cell line

CellTiter-Glo® Luminescent reagent was used to perform a cell viability assay. VCR was diluted at 2nM, 1nM, 0.5nM, 0.25nM, and 0.125nM in IMDM media and incubated with 5000 CHLA-258 cells per well. ETO was diluted at 1µg/mL, 0.5µg/mL, 0.25µg/mL, 0.125µg/mL, and 0.0625µg/mL.in IMDM media and incubated with 5000 CHLA-258 cells per well. The 96 round bottom plate was analyzed using a plate reader. Data was log-transformed to standard curve to determine the IC-50 concentration of VCR and ETO.

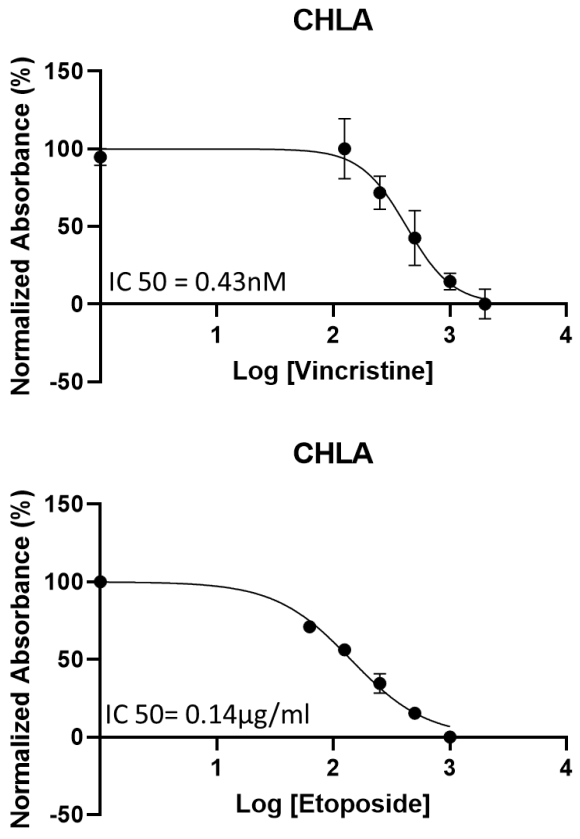

Figure 4.3

Increased LLT1 mRNA expression in non-treated EWS cell lines

Total RNA was isolated from EWS cell lines using a TRIzol reagent and cDNA was prepared using cDNA synthesis kit. LLT1 primers were then used to amplify LLT1 transcripts for 45 cycles. GAPDH was used as the endogenous control. The Jurkat cell line was used as a negative control as it has little to no expression of LLT1. Statistical analysis was performed using a student's t-test with a significant value set at (*) $p<0.05$ and (***) $p<0.001$.

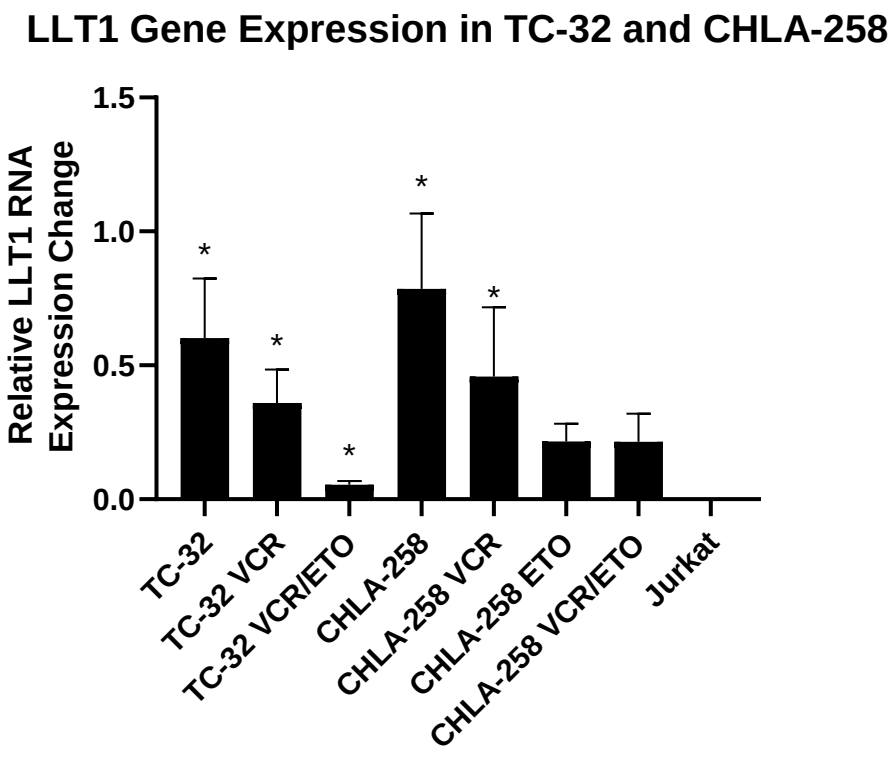

Figure 4.4

Treated EWS cell lines do not show a change in total LLT1 protein expression

An SDS-PAGE Bis-Tris gel was ran with cell samples TC-32, TC-32 VCR, TC-32 VCR/ETO, and CHLA-258 at 200V for 60 minutes followed by anti-LLT1 antibody incubation then followed by HRP-conjugated antibody incubation. Membrane was exposed to ECL substrate and imaged. Membrane was stripped then re-probed with anti-GAPDH-HRP antibody and exposed to ECL substrate and imaged. The quantification of band intensity is shown in the table below.

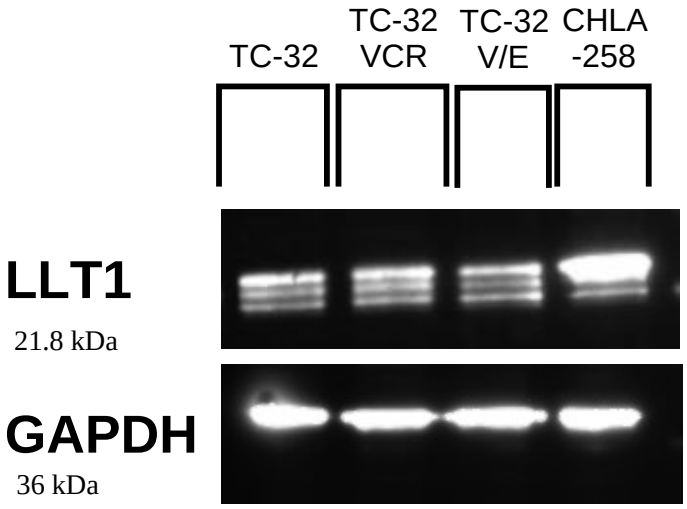

	Area	Mean intensity	Minimum	Maximum
TC-32	1248	157.148	10	255
TC-32+VCR	1248	157.142	20	255
TC-32+VCR+ETO	1248	143.624	22	255
CHLA-258	1248	237.510	42	255

Figure 4.5

LLT1 is expressed on the cell surface of TC-32 and CHLA-258 and treatment with vincristine further increases expression

Expression of LLT1 represented by median fluorescence intensity ratios was identified by flow cytometry analysis by staining EWS cell lines TC-32 and CHLA-258 with anti-LLT1-PE (tinted shade in histograms) or isotype IgG1-PE antibodies (unshaded in histograms).

One representative of all independent experiments shown next page.

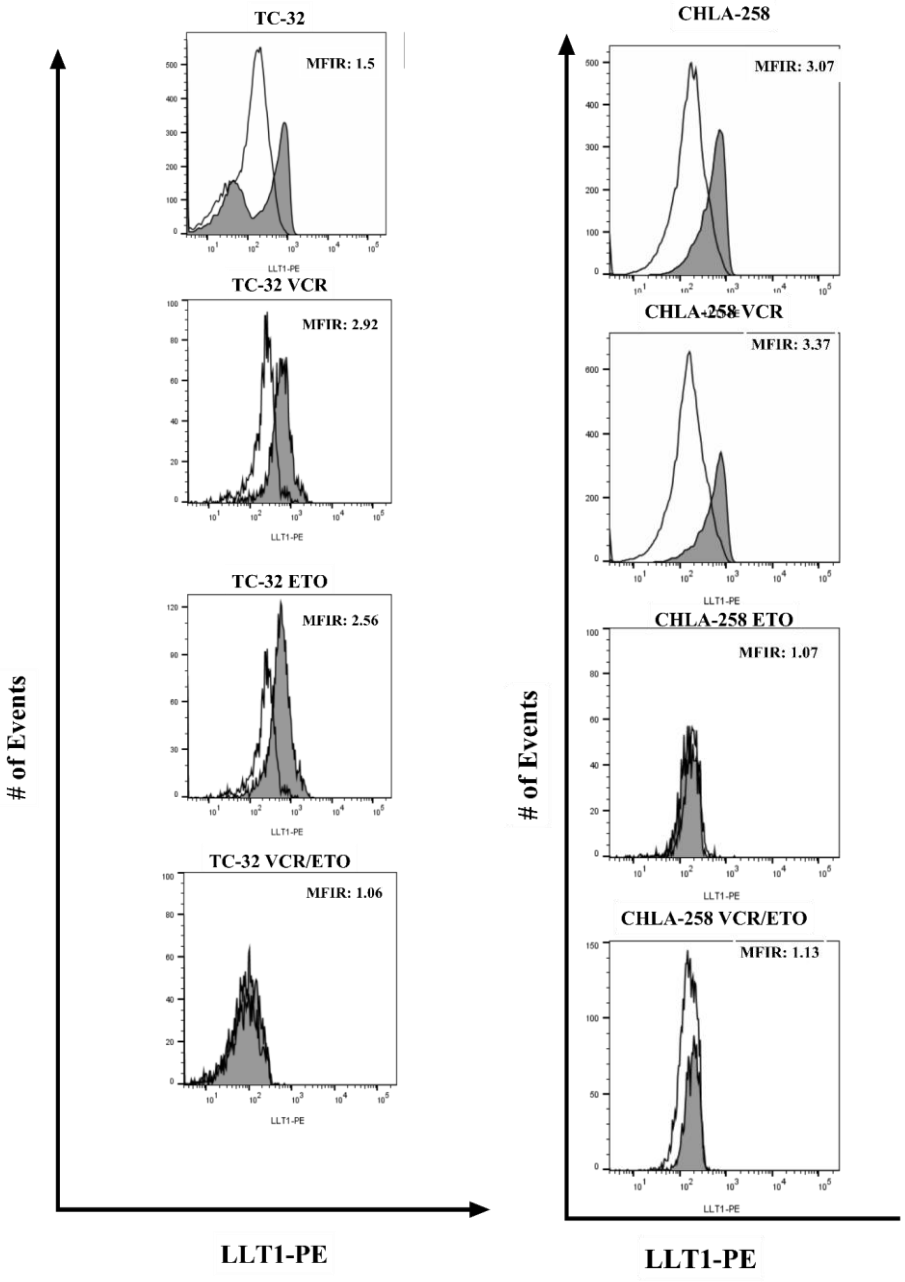
TC-32
MFIR: 1.5
TC-32 VCR
MFIR: 2.92
TC-32 ETO
MFIR: 2.56
TC-32 VCR/ETO
MFIR: 1.06
CHLA-258
MFIR: 3.07
CHLA-258 VCR
MFIR: 3.37
CHLA-258 ETO
MFIR: 1.07
CHLA-258 VCR/ETO
MFIR: 1.13
LLT1-PE
# of Events
LLT1-PE

Figure 4.6

Treatment of TC-32 cells with vincristine shows increased expression of LLT1

Flow cytometry was used to detect cell surface expression of LLT1 on TC-32 and CHLA-258 treated and non-treated cell lines. Mean fluorescence intensity ratio (MFIR) from independent experiments (n=3 for TC-32, TC-32 VCR, CHLA-258, and CHLA-258 VCR, n=1 for the other cell lines) were averaged. TC-32 VCR and CHLA-258 VCR both have higher averages than their control non-treated cell lines. A One-way ANOVA confirmed differences in the means of MFIRs at $p<0.05$ for all cell lines. Dunnett's multiple comparison post-hoc was used to test for statistical significance of MFIRs compared to the control TC-32 and CHLA-258 non-treated cell lines (* $p<0.05$, ** $p<0.001$).

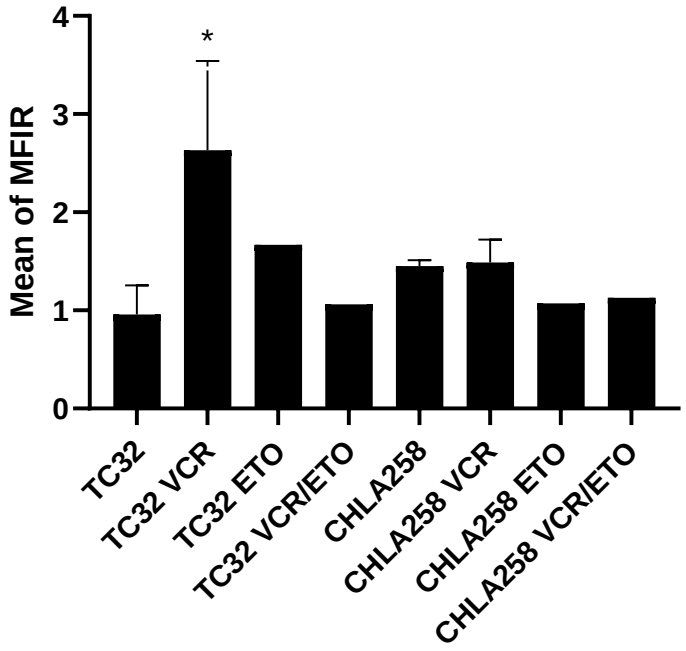

Specific Aim #2: Evaluate the cytolytic function of NK cells by blocking LLT1 on EWS cells.

Rationale

NK cells have the innate ability to target and lyse cells through the release of their lytic granules that contain factors such as granulysin, perforin, and granzyme. Through blocking the inhibitory ligand LLT1 on Ewing Sarcoma cells, NK cells can target Ewing Sarcoma cell in two ways. First, blocking of LLT1 with an antibody could tip the balance back in favor of activating signals thereby inducing an activation response from NK cells whereby lysis of the target cell occurs. Secondly, NK cells possess the CD16 (FcγRIII) receptor which can recognize the fragment chain (Fc) portion specific to the IgG antibody family. This will directly activate NK cells causing them to release their lytic granules. This process is known as antibody-dependent cellular cytotoxicity (ADCC). The objective of this aim is to treat the Ewing Sarcoma cells with a LLT1 blocking antibody and then evaluate the ability of NK cells to target and lyse those Ewing Sarcoma cells while blocking CD16 on NK cell to determine the cell specific effect of the LLT1-NKRP1A interaction on NK cell cytotoxicity. The working hypothesis is that blocking the LLT1-NKRP1A interaction with an anti-LLT1 mAb will lead to increased clearance of Ewing Sarcoma cells via increased cytotoxicity from NK cells.

4.2 LLT1 Expression Inhibits NK Cytotoxic Activity

4.2.1 Blocking LLT1-NKRP1A Interaction Leads to Increased NK Cell Cytotoxicity

A DELFIA cytotoxicity assay was performed in triplicates with target cells being the EWS treated and non-treated cell lines. Effector cells were isolated human NK cells from a PBMC sample. Briefly put, EWS cell lines were incubated with the BATDA reagent. After

incubation, the EWS cells were co-incubated with NK cells that were previously Fc blocked. The supernatant was taken from the sample and mixed with a Europium solution then analyzed using a plate reader. mIgG1 isotype control samples indicate that NK cells have a decreased ability to target and lyse LLT1 expressing EWS cells both treated and non-treated samples. Blocking the LLT1 receptor increased the cytotoxic ability of NK cells with an increase in specific cell lysis by utilizing an LLT1 antibody (R&D Systems, cat. # AF3480). TC-32 and TC-32 VCR cells lines showed similar cytotoxic efficacy when blocked with the anti-LLT1 antibody (~50%) at all E:T ratios. TC-32 had a % specific cell lysis of 49%, 48%, and 42% at a significance of p=0.009, 0.005, 0.0005, respectively (Figure 4.7). TC-32 VCR had a % specific cell lysis of 50%, 46%, and 46% at a significance of p=0.012, 0.0017, and 0.025, respectively. TC-32 ETO showed highly increased NK cell cytotoxic efficacy at % specific cell lysis of 160%, 152%, and 146% at a significance of p=0.008, 0.004, and 0.002, respectively. CHLA-258 had the highest NK cell cytotoxicity at 80% (25:1 ratio) with CHLA-258 VCR and CHLA-258 ETO showing good efficacy as well at comparable cell specific lysis percentages. CHLA-258 had a % specific cell lysis at 78%, 78%, and 73%, at a significance of p=0.0035, 0.0048, and 0.042, respectively. CHLA-258 VCR had a % specific cell lysis at 62%, 59%, and 60%, at a significance of p=0.005, 0.02, and 0.003, respectively. CHLA-258 ETO had a % specific cell lysis at 51%, 46%, and 46%, at a significance of p=0.006, 0.0009, and 0.005, respectively (Figure 4.7). Statistical significance was analyzed using a Student's T-test with a Welch's correction. Significance was set at (*) $p<0.05$, and (***) $p<0.001$.

Figure 4.7

Blocking LLT1-NKRP1A Interaction Leads to Increased NK Cell Cytotoxicity

Treated and non-treated EWS TC-32 and CHLA-258 samples were loaded with BATDA reagent then co-incubated with PBMC derived NK cells for 2 hours. The supernatant was analyzed after the incubation period by mixing it with a Europium solution and reading out the results on a plate reader. Samples were run in triplicates at various effector to target ratios (E:T) (i.e., 25:1, 5:1, 1:1). Statistical significance was analyzed using a Student's T-test with a Welch's correction. Significance was set at (*) $p<0.05$, and (***) $p<0.001$.

One representative graph of the independent experiment shown next page.

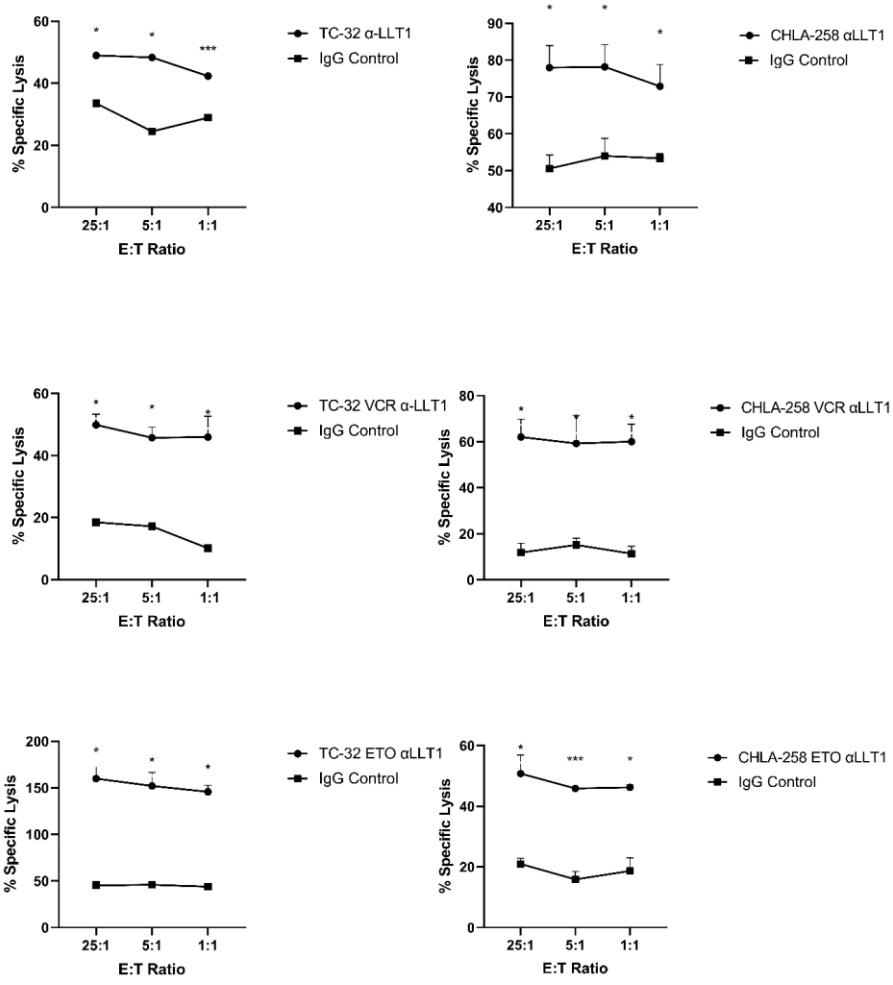
% Specific Lysis
E:T Ratio
25:1
5:1
1:1
TC-32 α-LLT1
IgG Control
CHLA-258 αLLT1
IgG Control
TC-32 VCR α-LLT1
IgG Control
CHLA-258 VCR αLLT1
IgG Control
TC-32 ETO αLLT1
IgG Control
CHLA-258 ETO αLLT1
IgG Control

CHAPTER V

DISCUSSION, CONCLUSION, AND LIMITATIONS

The expression of LLT1 on TC-32 and CHLA-258 cell lines is consistent with our previous findings that LLT1 is expressed on triple negative breast cancer (TNBC) and prostate cancer cell lines[92, 93]. Similarly, the cell surface expression of LLT1 is consistent with our previous findings[92, 93]. A new finding of this research shows that LLT1 is expressed on the cell surface of EWS cells and the expression is further increased in TC-32 cell line when treated with VCR. CHLA-258 LLT1 cell surface expression remained consistent, or slightly decreased in treated samples. Although cell surface expression is increased in TC-32 VCR treated cell line, there is a discrepancy with the RT-qPCR and western blot data. The RT-qPCR data indicated that the mRNA expression was decreased after treatment with vincristine and etoposide which is possible as not every RNA transcript translates to protein. Western blot data showed that the total LLT1 protein concentration in VCR treated TC-32 EWS cell line compared to untreated TC-32 did not change. Flow cytometry analysis shows that cell surface expression of LLT1 is increased in TC-32 and CHLA-258 cell lines as compared to the non-treated TC-32 and CHLA-258 cells based on the mean fluorescence intensity ratio (MFIR). Although the studies were not conducted in this project, previous data in prostate cancer cell lines showed increased cell surface LLT1 expression with some intracellular expression of LLT1 as compared to normal prostate cells showing more of intracellular LLT1 expression as compared to minimal or no expression on the cell surface[93]. Since LLT1 expression is expressed both intracellularly and on the surface of the cell membrane in prostate cancer cells, the same could be true for EWS cells. If LLT1 is expressed intracellularly and on the membrane surface in EWS cells, the discrepancy in RNA

expression and no change in total protein expression as indicated by the western blot data could be due to either 1) efficient translation of LLT1 into the functional protein, or 2) decreased regulatory mechanisms that inhibit overexpression of LLT1 transcripts, but traffic translated LLT1 protein to the cell surface. Current regulatory mechanisms of how LLT1 is trafficked to the cell surface and maintained within the cell are not known leaving a gap in our understanding of what is occurring. Furthermore, the expression of LLT1 on the surface of TC-32 and CHLA-258 indicates that LLT1 is present on the cell surface as a mechanism of immunosurveillance escape from NK cells whereby negative signals predominate over activating signals. This is also consistent with our previous data[92, 93]. Although expression of DNAM-1 and NKG2D was not analyzed in this study, a previous study conducted by Verhoeven *et al.*, showed that EWS are lysed directly through these activating receptors[120]. Therefore, blocking LLT1 could lead to increased cytotoxicity through DNAM-1 and NKG2D activating receptors.

The decrease in RNA expression in treated cells versus untreated cells is interesting but not surprising as not all of the RNA transcripts translate into expressed protein. We were interested in the relative RNA expression of LLT1 in these treated cell lines, but our most important goal was to determine the expression of LLT1 on the cell surface and determine its functional outcome. Flow cytometry showed that of the gated live cells, and compared to the isotype control, CHLA-258 VCR, CHLA-258 ETO, and CHLA-258 VCR/ETO had a $LLT1^+$ cell population of 63.0%, 3.11%, and 1.19% respectively. This indicates that LLT1 is expressed on the cell surface of these cell lines with treatment of chemotherapeutic drugs. A caveat to this is that for CHLA-258 ETO and CHLA-258 VCR/ETO cell lines were highly unstable and only one independent experiment of flow cytometry occurred for these samples.

From the flow cytometry results all cell samples had a distinct $LLT1^+$ population. From the representative graphs, TC-32, TC-32 VCR, TC-32 ETO, and TC-32 VCR/ETO had an $LLT1^+$ population of 75.7%, 60.0%, 43.3%, and 8.62, respectively. CHLA-258, CHLA-258 VCR, CHLA-258 ETO, and CHLA-258 VCR/ETO had an $LLT1^+$ population of 64.5%, 63.0%, 3.11%, and 1.19%, respectively. Cancer cell culture are not a homogenous culture and differential $LLT1^+$ cell population expression indicates that the cultured EWS samples consisted of a heterogenous population of cells. In future studies it will be interesting to see if LLT1 expression is correlated with expression of *EWSR1-FLI1* expression since the *EWSR1-FLI1* gene is differentially expressed in healthy patients.

Although our results show that LLT1 is expressed on treated and non-treated cell lines, the implementation of chemotherapeutic drugs in a monolayer system made samples such as TC-32 ETO, TC-32 VCR/ETO, CHLA-258 ETO, and CHLA-258 VCR/ETO highly unstable and difficult to perform any downstream applications. One method to circumvent this and have reproducible results that increase viability to mimic chemoresistance is change the culture method. 2D monolayer cell culture is the staple on *in vitro* studies but utilizing a 3D culture model would be beneficial because it would mimic the solid tumor of a EWS tumor[122, 123]. Another *in vitro* culture system that could be utilized is the Boyden's chamber which opens the possibility to study invasiveness and migration potential of tumor cells with the addition of other variables[122].

To further investigate how increased LLT1 expression affects EWS and NK cell interactions it is important to look at how cytotoxicity is affected. Previous cytotoxicity assays utilized loading target cells (in this case EWS cells) with radioactive isotopes like chromium 51 (Cr^{51}). In this study we utilized the DELFIA cytotoxicity assay which utilizes a non-radioactive

molecule that becomes fluorescent when combined with the lanthanide – europium. When this assay was performed at different effector to target ratios (E:T) such as 25:1, 5:1, and 1:1 we show that blocking LLT1 interaction through the NKRP1A receptor on NK cells leads to increased lysis of EWS cells with the largest percentage of lysis occurring at the 25:1 ratio compared to the isotype control. Consistently high percent specific lysis occurred in both treated and non-treated cell lines indicating that NK cells are effective at targeting EWS cells when the LLT1-NKRP1A interaction is blocked. This is also consistent with our previous data providing further evidence that when the LLT1-NKRP1A interaction is blocked, NK cell lysis increases partially restoring the delicate balance between inhibitory and activating signals[92, 93]. Interestingly, cytotoxicity assay data indicates that treated TC-32 and CHLA-258 with VCR and ETO have an increased cytolytic ability compared to the non-treated TC-32 and CHLA-258 cell lines. This is interesting for the TC-32 and CHLA-258 cell lines treated with ETO because our flow cytometry results suggest that LLT1 surface expression is slightly decreased. An explanation for this may be that since the total cell population that expressed LLT1 was slightly decreased, the blocking antibody concentration was sufficient to saturate any LLT1 expression which further increased the efficacy of NK cell mediated lysis. Due to the increased cytotoxicity in vincristine and etoposide treated TC-32 and CHLA-258 cell lines, studies should investigate the efficacy of NK cell to target EWS cells *in vivo* post, or during chemotherapeutic treatment.

For future studies it will be important to evaluate the efficacy of using LLT1 as a standalone monoclonal antibody therapy and as a combinatorial therapy in tandem with chemotherapy drugs. Based on the results of this study, treatment with vincristine to induce chemoresistance will be ideal and then use anti-LLT1 antibody treatment before starting chemotherapy in one group and starting it after chemotherapy in another group. Additionally,

picking the right mouse model will be important to consider. NUDE mice offer a potential route as they have deficient T cells and partially deficient B cells meaning that the efficacy of NK cells in response to EWS tumor cells *in vivo*. NSG mice offer another *in vivo* route of study, but additional considerations must be taken due to the null allele of the IL2 receptor common gamma chain (*IL2rγ*^{null}) meaning that the NK cell population in nonfunctional. To circumvent this NK cells could be adoptively transferred into the mice and activated via IL-15 or IL-2 prior to administration, or NK cells could be co-incubated with K562 feeder cells that have IL-15 expressed on the cell surface[124].

Additionally, the studies show that the EWS tumor mass is made up of a heterogenous group of cells with various mutational burdens[1, 125-127]. *EWSR1-FLI1* is also varied in expression within this heterogenous group of cells[1]. Knowing that *EWSR1-FLI1* expression is varied, it will be important to determine if LLT1^{+} expression is dependent on the varied expression of *EWSR1-FLI1* expression. It will also be important to determine the effect of administering VCR and ETO has on *EWSR1-FLI1* expression and if this acts in coordination with increased LLT1 expression or not. Determining this information will give valuable insight into how LLT1 expression is modified under these differing factors. Ultimately it will tell us if chemoresistance is contributing to immunoresistance in the EWS cells, or if varied expression of *EWSR1-FLI1* is contributing to the fitness of these cells and driving immunoresistance. This idea is taken from our flow cytometry data that showed distinct populations of LLT1^{+} and LLT1^{-} cells indicating that LLT1 is not ubiquitously expressed in EWS cells but does make up a distinct population of EWS cells. Knowing this *in-vitro* information will allow us to tailor the treatment of α-LLT1 monoclonal antibody treatment *in-vivo*.

Furthermore, a prevailing issue with *in-vivo* immunotherapy studies is sufficiently activating the NK cells without causing adverse side-effects[128-131]. IL-2 was commonly used but can over activate the immune system and can be very dangerous[132]. An alternative method that I suggest being used in our *in-vivo* studies is co-incubating NK cells with IL-15 to further activate the NK cells, then performing an adoptive transfer into the mice and analyze the results[120, 124, 133]. This will allow the NK cells to become activated since IL-15 is a potent activator and increased viability of NK cells while minimizing the side-effects of activating cytokines. Lastly, performing the same treatment in tandem with a TGFRβ inhibitory to ablate TGF-β signaling will be important to look at. Administration of TGF-β is shown to decrease the cytotoxicity potential of NK cells and suppress their effector function[133]. Inhibiting this signal pathway and adoptively transferring IL-15 activated NK cells would enhance their effector function while minimizing the effects of systemic treatment.

CONCLUSIONS AND LIMITATIONS

Lectin-Like Transcript-1 (LLT1) is an inhibitory ligand that is present in healthy tissues but is also known to be upregulated in various cancers. The expression and function of LLT1 in Ewing Sarcoma has not been performed in any known EWS cell lines nor patient samples. Here we determined the expression of LLT1 on two EWS cell lines harboring the *EWSR1-FLI1* gene fusion; TC-32 and CHLA-258. Chemotherapeutic drugs remain a treatment standard for EWS patients. Therefore, it is important to determine how chemotherapeutic drugs like vincristine and etoposide effect LLT1 expression. In this study we also used vincristine and etoposide by itself

and in combination to select for highly resistant cells through the application of selective pressures. Through flow cytometry analysis we determined that LLT1 expression is present on EWS cell line TC-32 and CHLA-258 and decreases when chemotherapeutic drugs are introduced expect in the case of TC-32 VCR and ETO. Similarly, using an NK cell cytotoxicity assays we determined that NK cells are efficient killers of EWS cell when treated with a blocking anti-LLT1 antibody. Our study showed that by blocking LLT1 on EWS cells NK cells were efficiently able to kill chemotherapy treated resistant EWS cells. Therefore, in future *in vivo* studies it will be important to treat mice with anti-LLT1 blockade both during and prior to chemotherapeutic treatment to determine its efficacy. In conclusion, LLT1 is expressed on EWS cell lines TC-32 and CHLA-258 and blockage of LLT1 leads to increased cytotoxicity via NK cell to target and clear EWS cells. Additionally, our data supports that for TC-32 and CHLA-258 treated cell lines, LLT1 expression is increased compared to non-treated TC-32 and CHLA-258 cells.

Although these studies show great promise in implementing LLT1 blockade to fight EWS, there are limitations to the conclusion of these studies. These studies lack to complete landscape of interactions that occur between EWS and NK cells. Additionally, this lacks the true complexity of the bone stroma and TME. Little information is present on the complete immune cell composition in EWS patients, but one common issue with solid tumors is the lack of TIL and the immunosuppressive TME. Therefore, it will be crucial to investigate ways to traffic lymphocytes – especially NK cells – to the TME without being suppressed by the TME. Caution should be used to extend the results of this study to human application. *In vivo* studies have yet to occur and until this model of treatment is established and well-studied in an organism, the

effect it has on human subject will remain to be seen and conclusions should not be extended to human application until *in vivo* studies conclude.

Abbreviations

NK cell: Natural Killer cell

EWS: Ewing Sarcoma

SEER: Surveillance epidemiology and end results

EWSR1: Ewing Sarcoma Breakpoint Region 1

TAF15: TATA-binding protein-associated factor 2N

FLI1: Friend leukemia virus integration site 1

ETV1: ETS Variant Transcription Factor 1

ETV4: ETS Variant Transcription Factor 4

GLI1: GLI Family Zinc Finger 1

FOXO1: Forkhead Box O1

CCK: Cholecystokinin

LOX: Protein-lysine 6-oxidase precursor

BAF: Barrier-to-autointegration

STEAP1: Six transmembrane epithelial antigen of prostate 1

NKX2.2: NK2 Homeobox 2

OTUD7A: OUT Deubiquitinase 7A

EYA3: EYA Transcriptional Coactivator and Phosphatase 3

IL-12: Interleukin 12

IL-15: Interleukin 15

MHC I: Major Histocompatibility Complex I

PD1: Programmed cell death protein 1

PD-L1: Programmed cell death ligand 1

TIL: Tumor Infiltrating Lymphocytes

VCR: Vincristine

ETO: Etoposide

PDX: Patient derived xenograft model

GSTM4: Glutathione S-Transferase Mu 4

TUBA1A: Tubulin Alpha 1a

TA: Tolfenamic Acid

TME: Tumor Microenvironment

Treg: Regulatory T cell

HLA-G: Human leukocyte antigen G

IL-6: Interleukin 6

TNF-α: Tumor Necrosis Factor alpha

PTH-rP: Parathyroid related Protein

TGF-β: Transforming Growth Factor beta

IGF-1: Insulin growth factor 1

PDGF: Platelet derived growth factor

RANKL/RANK: Receptor activator of nuclear factor kappa B ligand

OPG: Osteoprotegerin

OCIL: Osteoclast inhibitory ligand

LLT1: Lectin-like Transcript 1

PTX: Paclitaxel

ssGSEA: single-sample Gene Set Enrichment Analysis

NSG: NOD SCID gamma mouse

NUDE: Athymic nude mouse

CAR-T: Chimeric antigen receptor T cell

LINGO1: Leucine Rich Repeat and Ig Domain Containing 1

ROR1: Receptor Tyrosine Kinase Like Orphan Receptor 1

CAR-NK: Chimeric antigen receptor Natural Killer Cell

GD2: Disialoganglioside

References

1. Grünewald, T. G. P.; Cidre-Aranaz, F.; Surdez, D.; Tomazou, E. M.; de Álava, E.; Kovar, H.; Sorensen, P. H.; Delattre, O.; Dirksen, U., Ewing sarcoma. *Nature Reviews Disease Primers* **2018,** *4* (1), 5.

2. Ewing, J., Diffuse endothelioma of bone. *CA: A Cancer Journal for Clinicians* **1972,** *22* (2), 95-98.

3. Siegel, R. L.; Miller, K. D.; Jemal, A., Cancer statistics, 2020. *CA: A Cancer Journal for Clinicians* **2020,** *70* (1), 7-30.

4. Siegel, R. L.; Miller, K. D.; Jemal, A., Cancer statistics, 2018. *CA: A Cancer Journal for Clinicians* **2018,** *68* (1), 7-30.

5. Schaefer, K.-L.; Eisenacher, M.; Braun, Y.; Brachwitz, K.; Wai, D. H.; Dirksen, U.; Lanvers-Kaminsky, C.; Juergens, H.; Herrero, D.; Stegmaier, S.; Koscielniak, E.; Eggert, A.; Nathrath, M.; Gosheger, G.; Schneider, D. T.; Bury, C.; Diallo-Danebrock, R.; Ottaviano, L.; Gabbert, H. E.; Poremba, C., Microarray analysis of Ewing's sarcoma family of tumours reveals characteristic gene expression signatures associated with metastasis and resistance to chemotherapy. *European Journal of Cancer* **2008,** *44* (5), 699-709.

6. Balamuth Naomi, J. N., Ewing's sarcoma. *Lancet Oncology, The 11* (2), 184-92.

7. Jawad, M. U.; Cheung, M. C.; Min, E. S.; Schneiderbauer, M. M.; Koniaris, L. G.; Scully, S. P., Ewing sarcoma demonstrates racial disparities in incidence-related and sex-related differences in outcome. *Cancer* **2009,** *115* (15), 3526-3536.

8. Parkin, D. M.; Stiller, C. A.; Nectoux, J., International variations in the incidence of childhood bone tumours. *International Journal of Cancer* **1993,** *53* (3), 371-376.

9. Spector, L. G.; Hubbard, A. K.; Diessner, B. J.; Machiela, M. J.; Webber, B.; Schiffman, J. D., Comparative international incidence of Ewing sarcoma 1988 to 2012. *International Journal of Cancer n/a* (n/a).

10. Williams, L. A.; Richardson, M.; Kehm, R. D.; McLaughlin, C. C.; Mueller, B. A.; Chow, E. J.; Spector, L. G., The association between sex and most childhood cancers is not mediated by birthweight. *Cancer Epidemiol* **2018,** *57,* 7-12.

11. Burningham, Z.; Hashibe, M.; Spector, L.; Schiffman, J. D., The epidemiology of sarcoma. *Clin Sarcoma Res* **2012,** *2* (1), 14.

12. DeSantis, C. E.; Siegel, R. L.; Sauer, A. G.; Miller, K. D.; Fedewa, S. A.; Alcaraz, K. I.; Jemal, A., Cancer statistics for African Americans, 2016: Progress and opportunities in reducing racial disparities. *CA Cancer J Clin* **2016,** *66* (4), 290-308.

13. DeSantis, C. E.; Miller, K. D.; Goding Sauer, A.; Jemal, A.; Siegel, R. L., Cancer statistics for African Americans, 2019. *CA Cancer J Clin* **2019,** *69* (3), 211-233.

14. Schwartz, J. C.; Cech, T. R.; Parker, R. R., Biochemical Properties and Biological Functions of FET Proteins. *Annual Review of Biochemistry* **2015,** *84* (1), 355-379.

15. Hsu, T.; Trojanowska, M.; Watson, D. K., Ets proteins in biological control and cancer. *J Cell Biochem* **2004,** *91* (5), 896-903.

16. Sementchenko, V. I.; Watson, D. K., Ets target genes: past, present and future. *Oncogene* **2000,** *19* (55), 6533-6548.

17. Delattre, O.; Zucman, J.; Plougastel, B.; Desmaze, C.; Melot, T.; Peter, M.; Kovar, H.; Joubert, I.; de Jong, P.; Rouleau, G.; et al., Gene fusion with an ETS DNA-binding domain caused by chromosome translocation in human tumours. *Nature* **1992,** *359* (6391), 162-5.

18. Zucman, J.; Melot, T.; Desmaze, C.; Ghysdael, J.; Plougastel, B.; Peter, M.; Zucker, J. M.; Triche, T. J.; Sheer, D.; Turc-Carel, C.; et al., Combinatorial generation of variable fusion proteins in the Ewing family of tumours. *The EMBO journal* **1993,** *12* (12), 4481-4487.

19. Jeon, I. S.; Davis, J. N.; Braun, B. S.; Sublett, J. E.; Roussel, M. F.; Denny, C. T.; Shapiro, D. N., A variant Ewing's sarcoma translocation (7;22) fuses the EWS gene to the ETS gene ETV1. *Oncogene* **1995,** *10* (6), 1229-34.

20. Urano, F.; Umezawa, A.; Yabe, H.; Hong, W.; Yoshida, K.; Fujinaga, K.; Hata, J., Molecular analysis of Ewing's sarcoma: another fusion gene, EWS-E1AF, available for diagnosis. *Jpn J Cancer Res* **1998,** *89* (7), 703-711.

21. Riggi, N.; Suvà, M.-L.; Suvà, D.; Cironi, L.; Provero, P.; Tercier, S.; Joseph, J.-M.; Stehle, J.-C.; Baumer, K.; Kindler, V.; Stamenkovic, I., EWS-FLI-1 Expression Triggers a Ewing's Sarcoma Initiation Program in Primary Human Mesenchymal Stem Cells. *Cancer Research* **2008,** *68* (7), 2176.

22. Cidre-Aranaz, F.; Alonso, J., EWS/FLI1 Target Genes and Therapeutic Opportunities in Ewing Sarcoma. *Frontiers in oncology* **2015,** *5*, 162-162.

23. Boulay, G.; Sandoval, G. J.; Riggi, N.; Iyer, S.; Buisson, R.; Naigles, B.; Awad, M. E.; Rengarajan, S.; Volorio, A.; McBride, M. J.; Broye, L. C.; Zou, L.; Stamenkovic, I.; Kadoch, C.; Rivera, M. N., Cancer-Specific Retargeting of BAF Complexes by a Prion-like Domain. *Cell* **2017,** *171* (1), 163-178.e19.

24. Petermann, R.; Mossier, B. M.; Aryee, D. N. T.; Khazak, V.; Golemis, E. A.; Kovar, H., Oncogenic EWS-Fli1 interacts with hsRPB7, a subunit of human RNA polymerase II. *Oncogene* **1998,** *17* (5), 603-610.

25. Johnson, K. M.; Taslim, C.; Saund, R. S.; Lessnick, S. L., Identification of two types of GGAA-microsatellites and their roles in EWS/FLI binding and gene regulation in Ewing sarcoma. *PloS one* **2017,** *12* (11), e0186275-e0186275.

26. Markey, F. B.; Romero, B.; Parashar, V.; Batish, M., Identification of a New Transcriptional Co-Regulator of STEAP1 in Ewing's Sarcoma. *Cells* **2021,** *10* (6), 1300.

27. Üren, A.; Toretsky, J. A., Ewing's sarcoma oncoprotein EWS–FLI1: the perfect target without a therapeutic agent. *Future Oncology* **2005,** *1* (4), 521-528.

28. Su, S.; Chen, J.; Jiang, Y.; Wang, Y.; Vital, T.; Zhang, J.; Laggner, C.; Nguyen, K. T.; Zhu, Z.; Prevatte, A. W.; Barker, N. K.; Herring, L. E.; Davis, I. J.; Liu, P., SPOP and OTUD7A Control EWS–FLI1 Protein Stability to Govern Ewing Sarcoma Growth. *Advanced Science n/a* (n/a), 2004846.

29. Wang, Y.; Pandey, R. N.; Roychoudhury, K.; Milewski, D.; Kalin, T. V.; Szabo, S.; Pressey, J. G.; Hegde, R. S., Targeting EYA3 in Ewing Sarcoma Retards Tumor Growth and Angiogenesis. *Molecular Cancer Therapeutics* **2021,** *20* (5), 803.

30. Robin, T. P.; Smith, A.; McKinsey, E.; Reaves, L.; Jedlicka, P.; Ford, H. L., EWS/FLI1 Regulates EYA3 in Ewing Sarcoma via Modulation of miRNA-708, Resulting in Increased Cell Survival and Chemoresistance. *Molecular Cancer Research* **2012,** *10* (8), 1098.

31. Zöllner, S. K.; Amatruda, J. F.; Bauer, S.; Collaud, S.; de Álava, E.; DuBois, S. G.; Hardes, J.; Hartmann, W.; Kovar, H.; Metzler, M.; Shulman, D. S.; Streitbürger, A.; Timmermann, B.; Toretsky, J. A.; Uhlenbruch, Y.; Vieth, V.; Grünewald, T. G. P.; Dirksen, U., Ewing Sarcoma—Diagnosis, Treatment, Clinical Challenges and Future Perspectives. *Journal of Clinical Medicine* **2021,** *10* (8), 1685.

32. Kilpatrick, S. E.; Reith, J. D.; Rubin, B., Ewing Sarcoma and the History of Similar and Possibly Related Small Round Cell Tumors: From Whence Have We Come and Where are We Going? *Adv Anat Pathol* **2018,** *25* (5), 314-326.

33. Rademacher, M. J.; Cruz, A.; Faber, M.; Oldham, R. A. A.; Wang, D.; Medin, J. A.; Schloemer, N. J., Sarcoma IL-12 overexpression facilitates NK cell immunomodulation. *Scientific Reports* **2021,** *11* (1), 8321.

34. Holmes, T. D.; El-Sherbiny, Y. M.; Davison, A.; Clough, S. L.; Blair, G. E.; Cook, G. P., A Human NK Cell Activation/Inhibition Threshold Allows Small Changes in the Target Cell Surface Phenotype To Dramatically Alter Susceptibility to NK Cells. *The Journal of Immunology* **2011,** *186* (3), 1538.

35. Berghuis, D.; de Hooge, A. S.; Santos, S. J.; Horst, D.; Wiertz, E. J.; van Eggermond, M. C.; van den Elsen, P. J.; Taminiau, A. H.; Ottaviano, L.; Schaefer, K. L.; Dirksen, U.; Hooijberg, E.; Mulder, A.; Melief, C. J.; Egeler, R. M.; Schilham, M. W.; Jordanova, E. S.; Hogendoorn, P. C.; Lankester, A. C., Reduced human leukocyte antigen expression in advanced-stage Ewing sarcoma: implications for immune recognition. *J Pathol* **2009,** *218* (2), 222-31.

36. Machado, I.; López-Guerrero, J. A.; Scotlandi, K.; Picci, P.; Llombart-Bosch, A., Immunohistochemical analysis and prognostic significance of PD-L1, PD-1, and CD8+ tumor-infiltrating lymphocytes in Ewing's sarcoma family of tumors (ESFT). *Virchows Arch* **2018,** *472* (5), 815-824.

37. Spurny, C.; Kailayangiri, S.; Jamitzky, S.; Altvater, B.; Wardelmann, E.; Dirksen, U.; Hardes, J.; Hartmann, W.; Rossig, C., Programmed cell death ligand 1 (PD-L1) expression is not a predominant feature in Ewing sarcomas. *Pediatr Blood Cancer* **2018,** *65* (1).

38. Gidding, C. E. M.; Kellie, S. J.; Kamps, W. A.; de Graaf, S. S. N., Vincristine revisited. *Critical Reviews in Oncology/Hematology* **1999,** *29* (3), 267-287.

39. Yildiz, H.; Van Den Neste, E.; P. Defour, J.; Danse, E.; Yombi, J. C., Adult haemophagocytic lymphohistiocytosis: a review. *QJM: An International Journal of Medicine* **2020**.

40. Scopim-Ribeiro, R.; Lizardo, M. M.; Zhang, H. F.; Dhez, A. C.; Hughes, C. S.; Sorensen, P. H., NSG Mice Facilitate ex vivo Characterization of Ewing Sarcoma Lung Metastasis Using the PuMA Model. *Front Oncol* **2021,** *11*, 645757.

41. Ben-David, U.; Siranosian, B.; Ha, G.; Tang, H.; Oren, Y.; Hinohara, K.; Strathdee, C. A.; Dempster, J.; Lyons, N. J.; Burns, R.; Nag, A.; Kugener, G.; Cimini, B.; Tsvetkov, P.; Maruvka, Y. E.; O'Rourke, R.; Garrity, A.; Tubelli, A. A.; Bandopadhayay, P.; Tsherniak, A.; Vazquez, F.; Wong, B.; Birger, C.; Ghandi, M.; Thorner, A. R.; Bittker, J. A.; Meyerson, M.; Getz, G.; Beroukhim, R.; Golub, T. R., Genetic and transcriptional evolution alters cancer cell line drug response. *Nature* **2018,** *560* (7718), 325-330.

42. Fong, E. L. S.; Lamhamedi-Cherradi, S.-E.; Burdett, E.; Ramamoorthy, V.; Lazar, A. J.; Kasper, F. K.; Farach-Carson, M. C.; Vishwamitra, D.; Demicco, E. G.; Menegaz, B. A.; Amin, H. M.; Mikos, A. G.; Ludwig, J. A., Modeling Ewing sarcoma tumors in vitro with 3D scaffolds. *Proceedings of the National Academy of Sciences* **2013,** *110* (16), 6500-6505.

43. Lamhamedi-Cherradi, S.-E.; Santoro, M.; Ramammoorthy, V.; Menegaz, B. A.; Bartholomeusz, G.; Iles, L. R.; Amin, H. M.; Livingston, J. A.; Mikos, A. G.; Ludwig, J. A., 3D tissue-engineered model of Ewing's sarcoma. *Advanced Drug Delivery Reviews* **2014,** *79-80*, 155-171.

44. Hoffman, R. M., Patient-derived orthotopic xenografts: better mimic of metastasis than subcutaneous xenografts. *Nature Reviews Cancer* **2015,** *15* (8), 451-452.

45. Minas, T. Z.; Surdez, D.; Javaheri, T.; Tanaka, M.; Howarth, M.; Kang, H.-J.; Han, J.; Han, Z.-Y.; Sax, B.; Kream, B. E.; Hong, S.-H.; Çelik, H.; Tirode, F.; Tuckermann, J.; Toretsky, J. A.; Kenner, L.; Kovar, H.; Lee, S.; Sweet-Cordero, E. A.; Nakamura, T.; Moriggl, R.; Delattre, O.; Üren, A., Combined experience of six independent laboratories attempting to create an Ewing sarcoma mouse model. *Oncotarget; Vol 8, No 21* **2016**.

46. Mansoori, B.; Mohammadi, A.; Davudian, S.; Shirjang, S.; Baradaran, B., The Different Mechanisms of Cancer Drug Resistance: A Brief Review. *Adv Pharm Bull* **2017,** *7* (3), 339-348.

47. Zhuo, R.; Kosak, K. M.; Sankar, S.; Wiles, E. T.; Sun, Y.; Zhang, J.; Ayello, J.; Prestwich, G. D.; Shami, P. J.; Cairo, M. S.; Lessnick, S. L.; Luo, W., Targeting Glutathione S-transferase M4 in Ewing sarcoma. *Front Pediatr* **2014,** *2*, 83.

48. Horbach, L.; Sinigaglia, M.; Da Silva, C. A.; Olguins, D. B.; Gregianin, L. J.; Brunetto, A. L.; Brunetto, A. T.; Roesler, R.; De Farias, C. B., Gene expression changes associated with chemotherapy resistance in Ewing sarcoma cells. *Mol Clin Oncol* **2018,** *8* (6), 719-724.

49. Shelake, S.; Sankpal, U. T.; Eslin, D.; Bowman, W. P.; Simecka, J. W.; Raut, S.; Ray, A.; Basha, R., Clotam enhances anti-proliferative effect of vincristine in Ewing sarcoma cells. *Apoptosis* **2019,** *24* (1-2), 21-32.

50. Zöllner, S. K.; Selvanathan, S. P.; Graham, G. T.; Commins, R. M. T.; Hong, S. H.; Moseley, E.; Parks, S.; Haladyna, J. N.; Erkizan, H. V.; Dirksen, U.; Hogarty, M. D.; Üren,

A.; Toretsky, J. A., Inhibition of the oncogenic fusion protein EWS-FLI1 causes G(2)-M cell cycle arrest and enhanced vincristine sensitivity in Ewing's sarcoma. *Sci Signal* **2017,** *10* (499).

51. Gieryng, A.; Pszczolkowska, D.; Walentynowicz, K. A.; Rajan, W. D.; Kaminska, B., Immune microenvironment of gliomas. *Laboratory Investigation* **2017,** *97* (5), 498-518.

52. Stankovic, B.; Bjørhovde, H. A. K.; Skarshaug, R.; Aamodt, H.; Frafjord, A.; Müller, E.; Hammarström, C.; Beraki, K.; Bækkevold, E. S.; Woldbæk, P. R.; Helland, Å.; Brustugun, O. T.; Øynebråten, I.; Corthay, A., Immune Cell Composition in Human Non-small Cell Lung Cancer. *Frontiers in Immunology* **2019,** *9* (3101).

53. Brinkrolf, P.; Landmeier, S.; Altvater, B.; Chen, C.; Pscherer, S.; Rosemann, A.; Ranft, A.; Dirksen, U.; Juergens, H.; Rossig, C., A high proportion of bone marrow T cells with regulatory phenotype (CD4+CD25hiFoxP3+) in Ewing sarcoma patients is associated with metastatic disease. *International Journal of Cancer* **2009,** *125* (4), 879-886.

54. Spurny, C.; Kailayangiri, S.; Altvater, B.; Jamitzky, S.; Hartmann, W.; Wardelmann, E.; Ranft, A.; Dirksen, U.; Amler, S.; Hardes, J.; Fluegge, M.; Meltzer, J.; Farwick, N.; Greune, L.; Rossig, C., T cell infiltration into Ewing sarcomas is associated with local expression of immune-inhibitory HLA-G. *Oncotarget* **2017,** *9* (5), 6536-6549.

55. Redini, F.; Heymann, D., Bone Tumor Environment as a Potential Therapeutic Target in Ewing Sarcoma. *Frontiers in Oncology* **2015,** *5* (279).

56. Lissat, A.; Joerschke, M.; Shinde, D. A.; Braunschweig, T.; Meier, A.; Makowska, A.; Bortnick, R.; Henneke, P.; Herget, G.; Gorr, T. A.; Kontny, U., IL6 secreted by Ewing sarcoma tumor microenvironment confers anti-apoptotic and cell-disseminating paracrine responses in Ewing sarcoma cells. *BMC Cancer* **2015,** *15*, 552.

57. Wu, Q.; Zhou, X.; Huang, D.; Ji, Y.; Kang, F., IL-6 Enhances Osteocyte-Mediated Osteoclastogenesis by Promoting JAK2 and RANKL Activity In Vitro. *Cell Physiol Biochem* **2017,** *41* (4), 1360-1369.

58. Steeve, K. T.; Marc, P.; Sandrine, T.; Dominique, H.; Yannick, F., IL-6, RANKL, TNF-alpha/IL-1: interrelations in bone resorption pathophysiology. *Cytokine & Growth Factor Reviews* **2004,** *15* (1), 49-60.

59. Yates, A. J.; Gutierrez, G. E.; Smolens, P.; Travis, P. S.; Katz, M. S.; Aufdemorte, T. B.; Boyce, B. F.; Hymer, T. K.; Poser, J. W.; Mundy, G. R., Effects of a synthetic peptide of a parathyroid hormone-related protein on calcium homeostasis, renal tubular calcium reabsorption, and bone metabolism in vivo and in vitro in rodents. *J Clin Invest* **1988,** *81* (3), 932-938.

60. Teitelbaum, S. L., Bone Resorption by Osteoclasts. *Science* **2000,** *289* (5484), 1504.

61. Boyle, W. J.; Simonet, W. S.; Lacey, D. L., Osteoclast differentiation and activation. *Nature* **2003,** *423* (6937), 337-342.

62. Chirgwin, J. M.; Guise, T. A., Molecular Mechanisms of Tumor-Bone Interactions in Osteolytic Metastases. **2000,** *10* (2), 20.

63. Lacey, D. L.; Timms, E.; Tan, H. L.; Kelley, M. J.; Dunstan, C. R.; Burgess, T.; Elliott, R.; Colombero, A.; Elliott, G.; Scully, S.; Hsu, H.; Sullivan, J.; Hawkins, N.; Davy, E.; Capparelli, C.; Eli, A.; Qian, Y. X.; Kaufman, S.; Sarosi, I.; Shalhoub, V.; Senaldi, G.; Guo, J.; Delaney, J.; Boyle, W. J., Osteoprotegerin Ligand Is a Cytokine that Regulates Osteoclast Differentiation and Activation. *Cell* **1998,** *93* (2), 165-176.

64. Picarda, G.; Matous, E.; Amiaud, J.; Charrier, C.; Lamoureux, F.; Heymann, M. F.; Tirode, F.; Pitard, B.; Trichet, V.; Heymann, D.; Redini, F., Osteoprotegerin inhibits bone

resorption and prevents tumor development in a xenogenic model of Ewing's sarcoma by inhibiting RANKL. *J Bone Oncol* **2013,** *2* (3), 95-104.

65. Lau, Y. S.; Adamopoulos, I. E.; Sabokbar, A.; Giele, H.; Gibbons, C. L. M. H.; Athanasou, N. A., Cellular and humoral mechanisms of osteoclast formation in Ewing's sarcoma. *Br J Cancer* **2007,** *96* (11), 1716-1722.

66. Zhou, H.; Kartsogiannis, V.; Hu, Y. S.; Elliott, J.; Quinn, J. M. W.; McKinstry, W. J.; Gillespie, M. T.; Ng, K. W., A Novel Osteoblast-derived C-type Lectin That Inhibits Osteoclast Formation. *Journal of Biological Chemistry* **2001,** *276* (18), 14916-14923.

67. Hu, Y. S.; Zhou, H.; Myers, D.; Quinn, J. M.; Atkins, G. J.; Ly, C.; Gange, C.; Kartsogiannis, V.; Elliott, J.; Kostakis, P.; Zannettino, A. C.; Cromer, B.; McKinstry, W. J.; Findlay, D. M.; Gillespie, M. T.; Ng, K. W., Isolation of a human homolog of osteoclast inhibitory lectin that inhibits the formation and function of osteoclasts. *J Bone Miner Res* **2004,** *19* (1), 89-99.

68. Zheng, F.; Liang, H.; Liu, R.; Quan, J.-X.; Li, X.-X.; Dai, C.-L.; Guo, G.; Zhang, J.-Y.; Wang, B.-L., Parathyroid hormone-related protein regulates osteoclast inhibitory lectin expression via multiple signaling pathways in osteoblast-like cells. *Endocrine* **2009,** *35* (1), 47-56.

69. D'Angelo, S. P.; Shoushtari, A. N.; Agaram, N. P.; Kuk, D.; Qin, L.-X.; Carvajal, R. D.; Dickson, M. A.; Gounder, M.; Keohan, M. L.; Schwartz, G. K.; Tap, W. D., Prevalence of tumor-infiltrating lymphocytes and PD-L1 expression in the soft tissue sarcoma microenvironment. *Hum Pathol* **2015,** *46* (3), 357-365.

70. Bonaventura, P.; Shekarian, T.; Alcazer, V.; Valladeau-Guilemond, J.; Valsesia-Wittmann, S.; Amigorena, S.; Caux, C.; Depil, S., Cold Tumors: A Therapeutic Challenge for Immunotherapy. *Frontiers in immunology* **2019,** *10*, 168-168.

71. Idos, G. E.; Kwok, J.; Bonthala, N.; Kysh, L.; Gruber, S. B.; Qu, C., The Prognostic Implications of Tumor Infiltrating Lymphocytes in Colorectal Cancer: A Systematic Review and Meta-Analysis. *Scientific Reports* **2020,** *10* (1), 3360.

72. Geukes Foppen, M. H.; Donia, M.; Svane, I. M.; Haanen, J. B. A. G., Tumor-infiltrating lymphocytes for the treatment of metastatic cancer. *Mol Oncol* **2015,** *9* (10), 1918-1935.

73. Gao, G.; Wang, Z.; Qu, X.; Zhang, Z., Prognostic value of tumor-infiltrating lymphocytes in patients with triple-negative breast cancer: a systematic review and meta-analysis. *BMC Cancer* **2020,** *20* (1), 179.

74. Guven, D. C.; Kilickap, S.; Yildirim, H. C.; Ceylan, F.; Bas, O.; Dizdar, O., Chemoimmunotherapy for the salvage treatment of Ewing sarcoma: A case report. *J Oncol Pharm Pract* **2020**, 1078155220965677.

75. Xiao, B.; Liu, L.; Li, A.; Xiang, C.; Wang, P.; Li, H.; Xiao, T., Identification and Verification of Immune-Related Gene Prognostic Signature Based on ssGSEA for Osteosarcoma. *Frontiers in oncology* **2020,** *10*, 607622-607622.

76. Chen, H.; Song, Y.; Deng, C.; Xu, Y.; Xu, H.; Zhu, X.; Song, G.; Tang, Q.; Lu, J.; Wang, J., Comprehensive analysis of immune infiltration and gene expression for predicting survival in patients with sarcomas. *Aging (Albany NY)* **2020,** *13* (2), 2168-2183.

77. Zhou, Y.; Xu, B.; Wu, S.; Liu, Y., Prognostic Immune-Related Genes of Patients With Ewing's Sarcoma. *Front Genet* **2021,** *12*, 669549-669549.

78. Yee, D.; Favoni, R. E.; Lebovic, G. S.; Lombana, F.; Powell, D. R.; Reynolds, C. P.; Rosen, N., Insulin-like growth factor I expression by tumors of neuroectodermal origin with the t(11;22) chromosomal translocation. A potential autocrine growth factor. *J Clin Invest* **1990,** *86* (6), 1806-1814.

79. Grunewald, T. G. P.; Ranft, A.; Esposito, I.; da Silva-Buttkus, P.; Aichler, M.; Baumhoer, D.; Schaefer, K. L.; Ottaviano, L.; Poremba, C.; Jundt, G.; Jürgens, H.; Dirksen, U.; Richter, G. H. S.; Burdach, S., High STEAP1 expression is associated with improved outcome of Ewing's sarcoma patients. *Ann Oncol* **2012,** *23* (8), 2185-2190.

80. Town, J.; Pais, H.; Harrison, S.; Stead, L. F.; Bataille, C.; Bunjobpol, W.; Zhang, J.; Rabbitts, T. H., Exploring the surfaceome of Ewing sarcoma identifies a new and unique therapeutic target. *Proc Natl Acad Sci U S A* **2016,** *113* (13), 3603-8.

81. Maude, S. L.; Frey, N.; Shaw, P. A.; Aplenc, R.; Barrett, D. M.; Bunin, N. J.; Chew, A.; Gonzalez, V. E.; Zheng, Z.; Lacey, S. F.; Mahnke, Y. D.; Melenhorst, J. J.; Rheingold, S. R.; Shen, A.; Teachey, D. T.; Levine, B. L.; June, C. H.; Porter, D. L.; Grupp, S. A., Chimeric antigen receptor T cells for sustained remissions in leukemia. *N Engl J Med* **2014,** *371* (16), 1507-17.

82. Huang, X.; Park, H.; Greene, J.; Pao, J.; Mulvey, E.; Zhou, S. X.; Albert, C. M.; Moy, F.; Sachdev, D.; Yee, D.; Rader, C.; Hamby, C. V.; Loeb, D. M.; Cairo, M. S.; Zhou, X., IGF1R- and ROR1-Specific CAR T Cells as a Potential Therapy for High Risk Sarcomas. *PloS one* **2015,** *10* (7), e0133152-e0133152.

83. Kailayangiri, S.; Altvater, B.; Spurny, C.; Jamitzky, S.; Schelhaas, S.; Jacobs, A. H.; Wiek, C.; Roellecke, K.; Hanenberg, H.; Hartmann, W.; Wiendl, H.; Pankratz, S.; Meltzer, J.; Farwick, N.; Greune, L.; Fluegge, M.; Rossig, C., Targeting Ewing sarcoma with activated

and GD2-specific chimeric antigen receptor-engineered human NK cells induces upregulation of immune-inhibitory HLA-G. *Oncoimmunology* **2017,** *6* (1), e1250050.

84. Vitale, M.; Zimmer, J.; Castriconi, R.; Hanau, D.; Donato, L.; Bottino, C.; Moretta, L.; de la Salle, H.; Moretta, A., Analysis of natural killer cells in TAP2-deficient patients: expression of functional triggering receptors and evidence for the existence of inhibitory receptor(s) that prevent lysis of normal autologous cells. *Blood* **2002,** *99* (5), 1723-1729.

85. Fernandez, N. C.; Treiner, E.; Vance, R. E.; Jamieson, A. M.; Lemieux, S.; Raulet, D. H., A subset of natural killer cells achieves self-tolerance without expressing inhibitory receptors specific for self-MHC molecules. *Blood* **2005,** *105* (11), 4416-4423.

86. Abel, A. M.; Yang, C.; Thakar, M. S.; Malarkannan, S., Natural Killer Cells: Development, Maturation, and Clinical Utilization. *Frontiers in Immunology* **2018,** *9* (1869).

87. Cichocki, F.; Grzywacz, B.; Miller, J. S., Human NK Cell Development: One Road or Many? *Frontiers in Immunology* **2019,** *10* (2078).

88. Yu, J.; Mao, H. C.; Wei, M.; Hughes, T.; Zhang, J.; Park, I.-k.; Liu, S.; McClory, S.; Marcucci, G.; Trotta, R.; Caligiuri, M. A., CD94 surface density identifies a functional intermediary between the CD56bright and CD56dim human NK-cell subsets. *Blood* **2010,** *115* (2), 274-281.

89. Chiossone, L.; Dumas, P. Y.; Vienne, M.; Vivier, E., Natural killer cells and other innate lymphoid cells in cancer. *Nat Rev Immunol* **2018,** *18* (11), 671-688.

90. Phatarpekar, P. V.; Billadeau, D. D., Molecular regulation of the plasma membrane-proximal cellular steps involved in NK cell cytolytic function. *Journal of Cell Science* **2020,** *133* (5), jcs240424.

91. Morvan, M. G.; Lanier, L. L., NK cells and cancer: you can teach innate cells new tricks. *Nature Reviews Cancer* **2016,** *16* (1), 7-19.

92. Marrufo, A. M.; Mathew, S. O.; Chaudhary, P.; Malaer, J. D.; Vishwanatha, J. K.; Mathew, P. A., Blocking LLT1 (CLEC2D, OCIL)-NKRP1A (CD161) interaction enhances natural killer cell-mediated lysis of triple-negative breast cancer cells. *Am J Cancer Res* **2018,** *8* (6), 1050-1063.

93. Mathew, S. O.; Chaudhary, P.; Powers, S. B.; Vishwanatha, J. K.; Mathew, P. A., Overexpression of LLT1 (OCIL, CLEC2D) on prostate cancer cells inhibits NK cell-mediated killing through LLT1-NKRP1A (CD161) interaction. *Oncotarget* **2016,** *7* (42), 68650-68661.

94. Wilson, E. B.; El-Jawhari, J. J.; Neilson, A. L.; Hall, G. D.; Melcher, A. A.; Meade, J. L.; Cook, G. P., Human Tumour Immune Evasion via TGF-β Blocks NK Cell Activation but Not Survival Allowing Therapeutic Restoration of Anti-Tumour Activity. *PLOS ONE* **2011,** *6* (9), e22842.

95. Holt, D.; Ma, X.; Kundu, N.; Fulton, A., Prostaglandin E2 (PGE2) suppresses natural killer cell function primarily through the PGE2 receptor EP4. *Cancer Immunology, Immunotherapy* **2011,** *60* (11), 1577-1586.

96. Pietra, G.; Manzini, C.; Rivara, S.; Vitale, M.; Cantoni, C.; Petretto, A.; Balsamo, M.; Conte, R.; Benelli, R.; Minghelli, S.; Solari, N.; Gualco, M.; Queirolo, P.; Moretta, L.; Mingari, M. C., Melanoma Cells Inhibit Natural Killer Cell Function by Modulating the Expression of Activating Receptors and Cytolytic Activity. *Cancer Research* **2012,** *72* (6), 1407.

97. Cekic, C.; Day, Y.-J.; Sag, D.; Linden, J., Myeloid Expression of Adenosine A_{2A} Receptor Suppresses T and NK Cell Responses in the Solid Tumor Microenvironment. *Cancer Research* **2014,** *74* (24), 7250.

98. Waldhauer, I.; Goehlsdorf, D.; Gieseke, F.; Weinschenk, T.; Wittenbrink, M.; Ludwig, A.; Stevanovic, S.; Rammensee, H.-G.; Steinle, A., Tumor-Associated MICA Is Shed by ADAM Proteases. *Cancer Research* **2008,** *68* (15), 6368.

99. Larsen, S. K.; Gao, Y.; Basse, P. H., NK cells in the tumor microenvironment. *Crit Rev Oncog* **2014,** *19* (1-2), 91-105.

100. Bernardini, G.; Antonangeli, F.; Bonanni, V.; Santoni, A., Dysregulation of Chemokine/Chemokine Receptor Axes and NK Cell Tissue Localization during Diseases. *Frontiers in Immunology* **2016,** *7* (402).

101. Halama, N.; Braun, M.; Kahlert, C.; Spille, A.; Quack, C.; Rahbari, N.; Koch, M.; Weitz, J.; Kloor, M.; Zoernig, I.; Schirmacher, P.; Brand, K.; Grabe, N.; Falk, C. S., Natural Killer Cells are Scarce in Colorectal Carcinoma Tissue Despite High Levels of Chemokines and Cytokines. *Clinical Cancer Research* **2011,** *17* (4), 678.

102. Boles, K. S.; Barten, R.; Kumaresan, P. R.; Trowsdale, J.; Mathew, P. A., Cloning of a new lectin-like receptor expressed on human NK cells. *Immunogenetics* **1999,** *50* (1-2), 1-7.

103. Mathew, P. A.; Chuang, S. S.; Vaidya, S. V.; Kumaresan, P. R.; Boles, K. S.; Pham, H. T., The LLT1 receptor induces IFN-gamma production by human natural killer cells. *Mol Immunol* **2004,** *40* (16), 1157-63.

104. Rosen, D. B.; Bettadapura, J.; Alsharifi, M.; Mathew, P. A.; Warren, H. S.; Lanier, L. L., Cutting Edge: Lectin-Like Transcript-1 Is a Ligand for the Inhibitory Human NKR-P1A Receptor. *The Journal of Immunology* **2005,** *175* (12), 7796.

105. Aldemir, H.; Prod'homme, V.; Dumaurier, M. J.; Retiere, C.; Poupon, G.; Cazareth, J.; Bihl, F.; Braud, V. M., Cutting edge: lectin-like transcript 1 is a ligand for the CD161 receptor. *J Immunol* **2005,** *175* (12), 7791-5.

106. Kita, S.; Matsubara, H.; Kasai, Y.; Tamaoki, T.; Okabe, Y.; Fukuhara, H.; Kamishikiryo, J.; Krayukhina, E.; Uchiyama, S.; Ose, T.; Kuroki, K.; Maenaka, K., Crystal structure of extracellular domain of human lectin-like transcript 1 (LLT1), the ligand for natural killer receptor-P1A. *European Journal of Immunology* **2015,** *45* (6), 1605-1613.

107. Kamishikiryo, J.; Fukuhara, H.; Okabe, Y.; Kuroki, K.; Maenaka, K., Molecular basis for LLT1 protein recognition by human CD161 protein (NKRP1A/KLRB1). *J Biol Chem* **2011,** *286* (27), 23823-30.

108. Llibre, A.; Garner, L.; Partridge, A.; Freeman, G. J.; Klenerman, P.; Willberg, C. B., Expression of lectin-like transcript-1 in human tissues. *F1000Res* **2016,** *5*, 2929-2929.

109. Chalan, P.; Bijzet, J.; Huitema, M. G.; Kroesen, B.-J.; Brouwer, E.; Boots, A. M. H., Expression of Lectin-Like Transcript 1, the Ligand for CD161, in Rheumatoid Arthritis. *PloS one* **2015,** *10* (7), e0132436-e0132436.

110. Germain, C.; Meier, A.; Jensen, T.; Knapnougel, P.; Poupon, G.; Lazzari, A.; Neisig, A.; Håkansson, K.; Dong, T.; Wagtmann, N.; Galsgaard, E. D.; Spee, P.; Braud, V. M., Induction of lectin-like transcript 1 (LLT1) protein cell surface expression by pathogens and interferon-γ contributes to modulate immune responses. *The Journal of biological chemistry* **2011,** *286* (44), 37964-37975.

111. Braud, V. M.; Biton, J.; Becht, E.; Knockaert, S.; Mansuet-Lupo, A.; Cosson, E.; Damotte, D.; Alifano, M.; Validire, P.; Anjuère, F.; Cremer, I.; Girard, N.; Gossot, D.; Seguin-Givelet, A.; Dieu-Nosjean, M. C.; Germain, C., Expression of LLT1 and its receptor CD161 in lung cancer is associated with better clinical outcome. *Oncoimmunology* **2018,** *7* (5), e1423184.

112. Houchins, J. P.; Yabe, T.; McSherry, C.; Bach, F. H., DNA sequence analysis of NKG2, a family of related cDNA clones encoding type II integral membrane proteins on human natural killer cells. *Journal of Experimental Medicine* **1991,** *173* (4), 1017-1020.

113. Raulet, D. H.; Gasser, S.; Gowen, B. G.; Deng, W.; Jung, H., Regulation of ligands for the NKG2D activating receptor. *Annu Rev Immunol* **2013,** *31*, 413-41.

114. Ho, E. L.; Carayannopoulos, L. N.; Poursine-Laurent, J.; Kinder, J.; Plougastel, B.; Smith, H. R.; Yokoyama, W. M., Costimulation of multiple NK cell activation receptors by NKG2D. *J Immunol* **2002,** *169* (7), 3667-75.

115. Bottino, C.; Castriconi, R.; Pende, D.; Rivera, P.; Nanni, M.; Carnemolla, B.; Cantoni, C.; Grassi, J.; Marcenaro, S.; Reymond, N.; Vitale, M.; Moretta, L.; Lopez, M.; Moretta, A., Identification of PVR (CD155) and Nectin-2 (CD112) as cell surface ligands for the human DNAM-1 (CD226) activating molecule. *The Journal of experimental medicine* **2003,** *198* (4), 557-567.

116. Shibuya, A.; Campbell, D.; Hannum, C.; Yssel, H.; Franz-Bacon, K.; McClanahan, T.; Kitamura, T.; Nicholl, J.; Sutherland, G. R.; Lanier, L. L.; Phillips, J. H., DNAM-1, A Novel Adhesion Molecule Involved in the Cytolytic Function of T Lymphocytes. *Immunity* **1996,** *4* (6), 573-581.

117. Sloan, K. E.; Eustace, B. K.; Stewart, J. K.; Zehetmeier, C.; Torella, C.; Simeone, M.; Roy, J. E.; Unger, C.; Louis, D. N.; Ilag, L. L.; Jay, D. G., CD155/PVR plays a key role in cell motility during tumor cell invasion and migration. *BMC Cancer* **2004,** *4*, 73.

118. Sanchez-Correa, B.; Gayoso, I.; Bergua, J. M.; Casado, J. G.; Morgado, S.; Solana, R.; Tarazona, R., Decreased expression of DNAM-1 on NK cells from acute myeloid leukemia patients. *Immunol Cell Biol* **2012,** *90* (1), 109-15.

119. Casado, J. G.; Pawelec, G.; Morgado, S.; Sanchez-Correa, B.; Delgado, E.; Gayoso, I.; Duran, E.; Solana, R.; Tarazona, R., Expression of adhesion molecules and ligands for activating and costimulatory receptors involved in cell-mediated cytotoxicity in a large panel of human melanoma cell lines. *Cancer Immunol Immunother* **2009,** *58* (9), 1517-26.

120. Verhoeven, D. H.; de Hooge, A. S.; Mooiman, E. C.; Santos, S. J.; ten Dam, M. M.; Gelderblom, H.; Melief, C. J.; Hogendoorn, P. C.; Egeler, R. M.; van Tol, M. J.; Schilham, M. W.; Lankester, A. C., NK cells recognize and lyse Ewing sarcoma cells through NKG2D and DNAM-1 receptor dependent pathways. *Mol Immunol* **2008,** *45* (15), 3917-25.

121. Berghuis, D.; Schilham, M. W.; Vos, H. I.; Santos, S. J.; Kloess, S.; Buddingh, E. P.; Egeler, R. M.; Hogendoorn, P. C.; Lankester, A. C., Histone deacetylase inhibitors enhance expression of NKG2D ligands in Ewing sarcoma and sensitize for natural killer cell-mediated cytolysis. *Clin Sarcoma Res* **2012,** *2* (1), 8-8.

122. Kitaeva, K. V.; Rutland, C. S.; Rizvanov, A. A.; Solovyeva, V. V., Cell Culture Based in vitro Test Systems for Anticancer Drug Screening. *Front Bioeng Biotechnol* **2020,** *8*, 322-322.

123. Larsson, P.; Engqvist, H.; Biermann, J.; Werner Rönnerman, E.; Forssell-Aronsson, E.; Kovács, A.; Karlsson, P.; Helou, K.; Parris, T. Z., Optimization of cell viability assays to improve replicability and reproducibility of cancer drug sensitivity screens. *Scientific Reports* **2020,** *10* (1), 5798.

124. Phan, M. T.; Lee, S. H.; Kim, S. K.; Cho, D., Expansion of NK Cells Using Genetically Engineered K562 Feeder Cells. *Methods Mol Biol* **2016,** *1441*, 167-74.

125. Aynaud, M. M.; Mirabeau, O.; Gruel, N.; Grossetête, S.; Boeva, V.; Durand, S.; Surdez, D.; Saulnier, O.; Zaïdi, S.; Gribkova, S.; Fouché, A.; Kairov, U.; Raynal, V.; Tirode, F.; Grünewald, T. G. P.; Bohec, M.; Baulande, S.; Janoueix-Lerosey, I.; Vert, J. P.; Barillot,

E.; Delattre, O.; Zinovyev, A., Transcriptional Programs Define Intratumoral Heterogeneity of Ewing Sarcoma at Single-Cell Resolution. *Cell Rep* **2020,** *30* (6), 1767-1779.e6.

126. Katschnig, A. M.; Kauer, M. O.; Schwentner, R.; Tomazou, E. M.; Mutz, C. N.; Linder, M.; Sibilia, M.; Alonso, J.; Aryee, D. N. T.; Kovar, H., EWS-FLI1 perturbs MRTFB/YAP-1/TEAD target gene regulation inhibiting cytoskeletal autoregulatory feedback in Ewing sarcoma. *Oncogene* **2017,** *36* (43), 5995-6005.

127. Pedersen, E. A.; Menon, R.; Bailey, K. M.; Thomas, D. G.; Van Noord, R. A.; Tran, J.; Wang, H.; Qu, P. P.; Hoering, A.; Fearon, E. R.; Chugh, R.; Lawlor, E. R., Activation of Wnt/β-Catenin in Ewing Sarcoma Cells Antagonizes EWS/ETS Function and Promotes Phenotypic Transition to More Metastatic Cell States. *Cancer Res* **2016,** *76* (17), 5040-53.

128. Rezvani, K.; Rouce, R.; Liu, E.; Shpall, E., Engineering Natural Killer Cells for Cancer Immunotherapy. *Mol Ther* **2017,** *25* (8), 1769-1781.

129. Xie, G.; Dong, H.; Liang, Y.; Ham, J. D.; Rizwan, R.; Chen, J., CAR-NK cells: A promising cellular immunotherapy for cancer. *EBioMedicine* **2020,** *59*, 102975.

130. Fang, F.; Xiao, W.; Tian, Z., NK cell-based immunotherapy for cancer. *Semin Immunol* **2017,** *31*, 37-54.

131. Lee, D. A., Cellular therapy: Adoptive immunotherapy with expanded natural killer cells. *Immunol Rev* **2019,** *290* (1), 85-99.

132. Schwartz, R. N.; Stover, L.; Dutcher, J. P., Managing toxicities of high-dose interleukin-2. *Oncology (Williston Park)* **2002,** *16* (11 Suppl 13), 11-20.

133. Viel, S.; Marçais, A.; Guimaraes, F. S.-F.; Loftus, R.; Rabilloud, J.; Grau, M.; Degouve, S.; Djebali, S.; Sanlaville, A.; Charrier, E.; Bienvenu, J.; Marie, J. C.; Caux, C.; Marvel, J.; Town, L.; Huntington, N. D.; Bartholin, L.; Finlay, D.; Smyth, M. J.; Walzer, T.,

TGF-β inhibits the activation and functions of NK cells by repressing the mTOR pathway. *Science Signaling* **2016,** *9* (415), ra19-ra19.